T.C.

ERCİYES ÜNİVERSİTESİ

BİLİMSEL ARAŞTIRMA PROJELERİ

KOORDİNASYON BİRİMİ

ALTERED miRNA AND GENE EXPRESSION IS ASSOCIATED WITH THE SURVIVAL OF RUMINANT GRANULOSA CELLS UNDER OXIDATIVE STRESS

Proje No: FOA-2015-5655

Proje Türü

Öncelikli Alan Araştırma Projesi

SONUÇ RAPORU

Proje Yürütücüsü:

Md Mahmodul Hasan SOHEL

Ziraat Fakültesi/Zootekni Bölümü

Araştırmacının Adı Soyadı

Yusuf KONCA-Ziraat Fakültesi/Zootekni Bölümü

Mehmet Ulaş ÇINAR-Ziraat Fakültesi/Zootekni Bölümü

Korhan ARSLAN-Veteriner Fakültesi/ Genetik ABD

Bilal AKYÜZ-Veteriner Fakültesi/Genetik ABD

Serpil SARIÖKAN-Veteriner Fakültesi/ Genetik ABD

Eylül 2017

KAYSERİ

TEŞEKKÜR

Araştırma projesi olarak yürütülen bu çalışmada araştırma konusunun belirlenmesinde ve konunun planlanıp yürütülmesinde emek veren çok değerli proje ekibine,

Yrd.Doç.Dr. Md. Mahmodul Hasan SOHEL

Eylül 2017

İÇİNDEKİLER (CONTENTS)

ABSTRACT

Oxidative stress has been found to be essential during ovulation which also has detrimental effects on cell function, while microRNAs (miRNAs) are known as major regulators for genes involved in cell survival. On the other hand, sulforaphane (SFN) has received a great deal of research attention because of its ability to induce the production of a battery of antioxidant enzymes in certain concentrations through the activation of the Nuclear factor (erythroid-derived 2)-like 2 (Nrf2) signaling pathway, which may effectively neutralize reactive oxygen species (ROS) induced oxidative stress. However, a functional link between oxidative stress and miRNA expression changes in granulosa cells (GCs) during oxidative stress remains to be investigated as very little is known about the effects of ROS-modulated miRNAs on GC function in post oxidative stress condition. Therefore, the goal of this project is to investigate the effects of different concentration of SFN on activating protective pathways and quantify the expression level of certain mRNAs miRNAs, which are considered to be associated with the oxidative stress, in GCs *in vitro*. In addition, we evaluated several phenotypic parameters including cell viability, cytotoxicity, ROS accumulation, mitochondrial activity in the cells of control and treated group. Real-time quantitative PCR technique was used to measure the expression level of candidate mRNAs and ready to use miRNA PCR array (96-well) was used to identify differentially regulated miRNAs in stressed cells. The results showed that there was a dramatic loss of cell viability and higher cytotoxic effects of SFN on GCs at higher concentrations ($>15\ \mu M$). The expression of Nuclear factor (erythroid-derived 2)-like 2 (NRF2) increased significantly ($p<0.05$) with fold change ranged 3-8 in SFN treated GCs, whereas Kelch Like ECH Associated Protein 1 (KEAP1) expression was either downregulated or similar as control group under the same conditions. Moreover, the relative expression of the NRF2 downstream antioxidant genes (PRDX1, CAT, TXN1and SOD1) was found to be highly expressed (fold change ranging from 2-5, $p<0.05$) in SFN treated GCs compared to the untreated control. miRNA expression analysis showed that there was massive deregulation of miRNA expression due to oxidative stress. We found 27 miRNAs were differentially regulated in oxidatively stressed cells, of which 17 miRNAs are upregulated and remaining 10 miRNAs are downregulated. miRNA cluster analysis revealed that more than 50% miRNAs are acted as individual miRNAs while others are in different clusters. To identify the biological relevance of these differentially regulated miRNAs, we identified their target genes and the most affected pathways. MAPK is one of the pathways targeted by downregulated miRNAs which is known to be activated by downregulated miRNAs. On the other hand, focal adhesion, mTOR signaling

pathway, FoxO signaling pathway and axon guidance are the pathways affected by the upregulated miRNAs. Taken together, our results confirm that certain concentration of SFN is helpful to activate defense pathway in GCs and number of miRNAs are differentially regulated in GCs in response to the oxidative insult.

Key words: Oxidative stress; mRNA; miRNA; sulforaphane; Nrf2-pathway and antioxidant.

ÖZET

Ovülasyon esansındaki oksidatif stres esansiyel olmakla birlikte zarar verici de olduğu bilinmektedir ve miRNA'lar ge regülasyonun da rol oynayarak hücrelerin yaşamsal devamlılığında rol oynarlar. Diğer yandan sulforafin (SFN) NRF2 yolağını harekete geçirerek antioksidan enzimlerin üretilmesini ve reaktif oksijen çeşitlerinin neden olduğu oksidatif stresinde azaltma sağlaması nedeniyle araştırıcıların ilgisini çekmektedir. Fakat granülosa hücrelerinin oksidatif stres esnasında miRNA'lar ile birlikte nasıl etkileim içinde olduklarına dair bilgiler çok azdır. Bu nedenle bu çalışmanın amacı farklı konsantrasyon seviyesindeki SFN nin in vitro granüloza hücrelerindeki oksidatif stresle ilişkisi bulunan genlerin mRNA larını ve miRNA ekspresyonlarını ortaya koymaktır. Onun dışında muamele ve kontrol grubunda bulunan hücrelerde hücre yaşam fonksiyonu, sitotoksite, ROS akümülasyonu gibi fenotiplere de bakılmıştır. Strese maruz kalmış hücrelerde miRNA ve mRNA profilleri Real-Time PCR kullanılarak belirlenmiştir. Sonuçlar granüloz hücrelerinde SFN nin yüksek dozlarında (>15 µM) hücrelerin yaşama güçlerinin azaldığını ve toksik etki yaptığını göstermiştir. NRF2 ekspresyonu SFN ile muamele edilmiş GC'lerde 3-8 kat artarken, KEAP1 ekspresyonu azalmış veya kontrol seviyesinde kalmıştır. Bununla birlikte SFN ile muamele edilmiş GC'lerde NRF2 ile ilişkisi bulunan antioksidan genlerinin (PRDX1, CAT, TXN1 ve SOD1) ekspresyonlarında artış gözlenmiştir. miRNA analizi muamele grubunda massif deregülasyonun olduğunu göstermiştir. İki grup arasında 27 adet miRNA farklılaşmış olup 17 tanesi upregülasyon 10 tanesi down regülasyon göstermiştir. miRNA ların biyolojik fonksiyonlarını göstermek için miRNA'ların hedef genleri ve biyolojik yolakları incelenmiştir. MAPK gen yolağının en çok down regüle miRNA lar tarafından hedeflenen yolak olduğu görülmüştür. Focal adhesion, mTOR signaling yolağı, FoxO signaling yolağı and axon guidance up-regüle olan miRNA lardan etkilenmiştir. Çalışma sonunda belirli SFN seviyesinin hücreleri oksidatif stresten koruduğu ve bunun da bazı miRNA ve mRNA lar sayesinde olduğu gözlenmiştir.

Anahtar kelimeler: Oksidatif stres; mRNA; miRNA; sülforafan; Nrf2 yolu ve antioksidan.

1. Introduction

GCs are the major cellular component in an ovarian follicular microenvironment and serve diverse indispensable functions during follicular growth and ovulation (Sohel and Cinar, 2015). Shortly before ovulation, a massive luteinizing hormone (LH) surge provokes GCs to differentiate into luteal cells. Progesterone synthesis in GCs is orchestrated by steroidogenic acute regulatory (StAR) protein, whose expression is known to be modulated by LH surge (Dou et al., 2016; Johnson et al., 2002). Furthermore, progesterone synthesized by luteinizing GCs is essential for the formation of the corpus luteum and maintenance of pregnancy. After the LH surge, inflammatory cells (e.g. vascular endothelial cells, macrophages, and neutrophils) are massively recruited at the site of follicular rupture and produce an excessive amount of ROS which causes acute inflammation, facilitate follicular rupture, and ovulation (Jabbour et al., 2009; Shkolnik et al., 2011). It also suggests that GCs are exposed to an elevated level of ROS during ovulation. On the other hand, in follicular atresia, apoptosis in GCs commenced by oxidative stress, partly due to the overproduction of ROS which is supported by the fact that macrophages are found in the follicular fluid of the atretic follicle (Loukides et al., 1990).

The Imbalance between the production of ROS and the ability of antioxidants to scavenge them potentially creates a condition known as oxidative stress (Rahal et al., 2014; Sies, 1997). Despite their significant role in living organisms, excessive generation of ROS is potentially responsible for a range of disorders and diseases including heart diseases, muscle degeneration, and cancer (Alfadda and Sallam, 2012; Brieger et al., 2012). Immediately after production, ROS can interact with all biological macromolecules near or at the site of their production and are generally involved in the peroxidative degradation of proteins and lipids which potentially leads to the destruction of the cell membrane, loss of mitochondrial activity, degradation of cellular structure and finally cells and tissue damage (Szczubial et al., 2015). Importantly, the endogenous defense system against ROS, i.e. a team of enzymatic antioxidants, such as superoxide dismutase (SOD), catalase (CAT), and glutathione peroxidase (GSH-Px) (Michiels et al., 1994), and non-enzymatic antioxidants including vitamin C, vitamin E, melatonin, albumin, and uric acid are found in the follicles which can scavenge excessive ROS and restore homeostasis.

The enzymatic antioxidant defense mechanism is a very complex process in which the Nrf2-ARE antioxidant pathway plays a central role in inducing the transcription of phase II antioxidant enzyme genes (Kang et al., 2005; Zhang et al., 2013). Under the homeostatic

condition, Nuclear factor (erythroid-derived 2)-like 2 (NRF2) remains inactive by binding with Kelch Like ECH Associated Protein 1 (KEAP1) and Cullin-3 and has a very short half-life (around 20 min) in the cytoplasm. However, under oxidative stress condition, electrophiles signal the disruption of the KEAP1-NRF2 bond and NRF2 is translocated to the nucleus. In the nucleus, NRF2 first interacts with small Maf proteins to form a heterodimer (Itoh et al., 1997), which later binds with antioxidant response element (ARE) and initiate the transcription of an array of antioxidative genes including peroxiredoxin-1 (*PRDX1*), catalase (*CAT*), superoxide dismutases (*SODs*) and thioredoxin-1 (*TXN*). NRF2-ARE pathway has been shown to be played an important role against atrazine-induced oxidative stress mediated damages in mouse ovarian tissues (Zhao et al., 2014). In addition, deletion of NRF2 transcription factor results reduced the number of ovarian follicles and accelerates ovarian aging in mice (Lim et al., 2015). However, the role of the NRF2-ARE pathway in granulosa cell apoptosis and proliferation is not completely understood. Many compounds including oltipraz, curcumin, SFN, and 3H-1, 2-dithiole-3-thione are well-known inducers of the Nrf2-ARE pathway (Kensler et al., 2013). Among these, SFN clearly stands out as one of the most potent inducers of the Nrf2-ARE signaling pathway (Guerrero-Beltrán et al., 2012).

SFN is a dietary isothiocyanate produced by the vegetables of the genus *Brassica* such as cabbage, brussels sprouts and broccoli (Guerrero-Beltrán et al., 2012). SFN induces Nrf2 signaling through thiocarbamylation at Cys151 resulting the disruption of the NRF2-KEAP1 binding and inhibition of NRF2 ubiquitination, followed by translocation to the nucleus and promote the transcription of phase II antioxidative genes (Kensler et al., 2013). In addition, SFN also enhances the induction of the survival signaling proteins such as B-cell lymphoma 2 (BCL2) and downregulates the proteins of death signaling pathway (Mukherjee et al., 2010).

microRNAs (miRNAs) are endogenously initiated non-coding RNA species of 18-22 nucleotide long and are considered as one of the major post-transcriptional regulators of gene expression (Hossain et al., 2012). By an imperfect binding to the 3′-untranslated region (3′ UTR) of target mRNA, miRNAs inhibit their function either by translational repression or by mRNA destabilization, or both (Wahid et al., 2010). Recent evidence suggests that miRNAs are not only present in cellular microenvironment but also present in various bio-fluids (Sohel, 2016). They are estimated to comprise 1-5% of animal genes and around 60% of mammalian protein coding genes are post-transcriptionally regulated by miRNAs (Afonso-Grunz and Müller, 2015).

Since their discovery, miRNAs have been found to be involved in many biological processes including proliferation, differentiation, development, and apoptosis. In addition, aberrant miRNA expression has been shown to be associated with many diseases such as cancer (Peng and Croce, 2016), diabetics (Simpson et al., 2016) cardiovascular disease (Romaine et al., 2015), and reproductive functions (Tesfaye et al., 2017). Furthermore, ample studies demonstrated the involvement of miRNAs in ovarian development (Khan et al., 2015), folliculogenesis (Baley and Li, 2012; Donadeu et al., 2012), oocyte cumulus expansion (Li et al., 2016), oocyte maturation (Pan et al., 2015), and early embryonic development (Laurent, 2008). We previously reported that excessive level of ROS produced by H_2O_2 was extremely cytotoxic to GCs in cell culture and caused higher cell death (Sohel et al., 2017). However, very little is known about the role of miRNAs in GCs during ovulation when oxidative stress usually takes place. Therefore, this study was conducted to

a) Investigate the effects of different concentration of SFN in activating survival pathways in GCs by quantifying candidate genes and other molecular markers.

b) Analyse the expression of miRNAs which are supposed to be differentially regulated under oxidative stress.

c) Identify the biological relevance of these differentially regulated miRNAs.

2. Materials and Methods

2.1. Collection of ovary and GCs

Bovine ovaries (n = 100, from ~ 60 females) were collected from the local slaughterhouse after the official permission given by the slaughterhouse management to use samples only for research purpose. Ovaries were kept in 0.9% saline solution at 38°C in a thermo-flask and transported to the laboratory within 2 h of collection. In the laboratory, ovaries were first washed three times with pre-warmed 0.9% saline solution and then dipped into 70% ethanol for 1 min. Following additional three washes with saline solution, ovaries were kept in warm DMEM/F-12 medium (Sigma Aldrich, D5546-6X500ML, St. Louis, MO) supplemented with penicillin (100 U/mL) and streptomycin (100 µg/mL) (Sigma-Aldrich, P4333, Steinheim, Germany). The follicular materials (follicular fluid containing GCs) were aspirated by 18-gauge needle attached to a 5-mL syringe form mature preovulatory follicles (13-18 mm in diameter) and placed into a 50-mL sterile Falcon tube containing 15 mL DMEM/F-12 medium supplemented with penicillin (100 U/mL) and streptomycin (100 µg/mL). Oocyte cumulus complex and cellular debris were allowed to settle down and the upper liquid, which contains the GCs, was transferred to a 15-mL tube and centrifuged at $500 \times g$ for 7 min.

2.2. GC culture, H_2O_2, and SFN treatment

GCs were collected and cultured according to the previous protocol (Sohel et al., 2013). Briefly, GC pellets were resuspended in 1 mL of red blood cell lysing solution (8.26 g/L NH4Cl) for 1 min to remove erythrocytes. Immediately after incubation 5 mL of DMEM/F-12 media containing 10% FBS was added in order to restore the isotonicity. After two additional washes with DMEM/F-12 media approximately 5×10^4, 1.5×10^5, and 6×10^5 viable cells were seeded in the 8-well chamber slide, 24-well and 6-well culture plates, respectively, containing DMEM/F-12 medium supplemented with 10% FBS (Pan-Biotech GmbH, P30-8500, Aidenbach, Germany), penicillin (100 U/mL) and streptomycin (100 µg/mL) at 37°C in a humidified atmosphere of 5% CO2 until 50-60% confluence. To investigate the effect of SFN, primary cultures of GCs were exposed to 0.05% DMSO (Miltenyi Biotec GmbH, Teterow, Germany) or different concentration of SFN (1-80 µM) (Sigma Aldrich, S4441-5MG, St. Louis, MO) for 24 h under culture condition. Based on the phenotypic evaluation of treated cells, three concentrations (low, medium and high) out of eight concentrations were chosen for further investigations. Following treatment, cells were investigated for their phenotypic characteristics or harvested using Trypsin EDTA (Biological Industries, cat no. 03-052-1B, Kibbutz Beit

Haemek, Israel) for genetic analysis. To induce oxidative stress, primary cultures of GCs were exposed to 75 µM H_2O_2 (Sigman-Aldrich) in culture media for 6 h under optimum culture conditions. This concentration was selected based on our experiences in the lab (Sohel et al., 2016). Following the treatments, cells were either investigated for different morphological characteristics or harvested using trypsin EDTA and stored in -80°C for further genetic analysis.

2.3. Cell Morphology and viability

Untreated control (0.05% DMSO treated) and SFN-exposed GCs were routinely observed under an inverted microscope (Nikon Eclipse TS100, Tokyo, Japan) throughout the experiment for morphological changes and confluence. The viability of cells was determined as previously described (Strober, 2001) with some modifications. Briefly, after the incubation period, both adherent and floating cells were collected and resuspended in 1 mL of the complete medium by gentle pipetting. Following that, 100 µl of cell suspension and 100 µl of 0.4% trypan blue were mixed into a micro-centrifuge tube and allowed to incubate for 1-2 min at room temperature. 10 µl of cell mixture/trypan blue was applied to the hemocytometer and placed under a microscope for counting live and dead cells. The percentage of viable cells was calculated as follows: percentage of cell viability = (number of unstained cells/number of total cells) × 100.

2.4. Cytotoxicity assay

Cytotoxic effect of different concentrations of SFN was determined using Cell Proliferation Reagent WST-1 (Roche Diagnostics GmbH, Mannheim, Germany) kit according to the manufacturer's protocol. Briefly, 1×104 viable GCs were plated in each well of 96-well microplate (flat bottom, tissue culture grade, Corning Incorporated, New York, USA) containing 100 µl/well culture medium and continue culture for 24 h in a humidified atmosphere (37°C and 5% CO2). Old media of each well was replaced by new media containing different concentrations of SFN (0-80 µM) and cultured for another 24 h. Following the culture period, 10 µl WST-1 reagent was added to each well of the microplate and incubated for 5 h at 37°C with the presence of 5% CO2. Following the incubation period, the microplate was shaken for 1 min and absorbance was measured using a microplate (ELISA) reader (Glomax Multi Detection System, Promega Bio Systems Sunnyvale, CA, USA) with the wavelength range of

460 nm. Blank measurements were obtained from wells containing only culture medium and used for normalization.

2.5. Extraction of total RNA and cDNA synthesis

Total RNA was extracted from GCs using the miRNeasy mini kit (Qiagen, Hilden, Germany) according to the manufacturer's instruction. An on-column DNase digestion step using RNase-Free DNase set (Cat no. 79254, Qiagen, Hilden, Germany) was performed during total RNA isolation in order to remove any additional DNA contamination. Purity and concentration of Total RNA were determined by a BioSpec-nano spectrophotometer (Shimadzu Biotech, Japan). The RNA was then reverse transcribed to cDNA using Maxima H Minus First Strand cDNA Synthesis Kit (Thermo Scientific, Massachusetts, USA) according to the manufacturer's instruction. The cDNA synthesis reaction consists of 5× RT Buffer (4 µl), 10 mM dNTP mix (1 µl), Maxima H Minus Enzyme mix (1µl), and oligo dT and random hexamer primers (0.25µl each). First, oligo dT, Random primer, and dNTP were added to the 200 ng of total RNA and the reaction volume was adjusted to 15 µl by adding nuclease free water and incubated at 65°C for 5min. After that, other components were added to the mixture and incubated for 10 min at 25°C followed by 15 min at 50°C and the reaction was terminated by heating at 85°C for 5 min.

2.6. Intracellular ROS accumulation

Accumulation of intracellular ROS in untreated control (0.05% DMSO treated) and SFN treated GCs were assessed by the fluorescent dye 2′7′-dichlorodihydrofluorescein diacetate (H2DCFDA; Molecular Probes, Eugene, OR) according to the manufacturer's protocol. Briefly, GCs from each group were first washed two times with DPBS and then 400 µl of 15 µM H2DCFDA was added to each well of 24-well culture plate and incubated for 30 min in dark at 37°C. Following the incubation cells were washed twice with PBS, and images were captured immediately under a fluorescence microscope (Nikon Eclipse Ti-S microscope, Nikon Instruments Inc., Tokyo, Japan) using a green-fluorescence filter. Mean fluorescence intensity of five non-overlapping fields per well was measured using ImageJ software.

2.7. Accumulation of lipid droplets

Accumulation of lipid droplets in SFN treated GCs were assessed using Oil Red O stain (Sigma Aldrich, O1391, St. Louis, MO) using manufacturer's protocol. Briefly, approximately 1.5×105 viable GCs were added to each well of 24-well culture plate and grown up to 50-60% confluence. After that various concentration of SFN was added to cells and continue the culture for another 24 h. Following the incubation period, media was completely removed and cells were washed two times with PBS and fixed in 10% formalin for 30 min at room temperature. Immediately prior to the staining, Oil red working solution was prepared and then incubated with cells for 40 min at room temperature. Following staining, cells were washed three times with distilled water and visualized by Leica DMIL LED inverted microscope (Leica microsystem Ltd., Germany).

2.8. Mitochondrial activity

The activity of mitochondria was examined using MitoTracker1 Red CMXRos (M7512; Life Technologies, Oregon, USA) using manufacturer's protocol. Briefly, GCs from different treatment groups were washed twice with DPBS and then 100 nM Mito Tracker red dye was added and incubated for 45 min. GCs were then washed two times with DPBS and were fixed overnight with 4% formaldehyde. In the next day, fixed cells were mounted with Vectashield Mounting Medium with DAPI (H-1200, Vector Laboratories, Inc., CA, USA). Images were acquired by a fluorescence microscope (Nikon Eclipse Ti-S microscope, Nikon Instruments Inc., Tokyo, Japan) using a red-fluorescence filter. Mean fluorescence intensity of five non-overlapping fields in each well was measured using ImageJ software.

2.9. Detection of apoptosis using TUNEL assay

Apoptosis in GCs was analyzed by Terminal deoxynucleotidyl transferase (TdT) dUTP Nick-End Labeling (TUNEL) assay using Click-iT® Plus TUNEL Assay kit (Life Technologies, Inc., Carlsbad, CA, USA) according to manufacturer's instruction. In brief, at the end of the indicated treatments, 50 µL of TdT reaction mixture was added to each well of 96-well plates and incubated for 1 h at 37°C, followed by 30 min incubation with the Alexa Fluor® 594 dye (red fluorescence). Then, the cells were counterstained with 5 ng/mL DAPI (ThermoFisher Scientific) in PBS for 10 min and observed under a fluorescence microscope (Nikon Eclipse

Ti-S microscope, Nikon Instruments Inc., Tokyo, Japan) using a red-fluorescence filter. The TUNEL-positive nuclei of five non-overlapping fields per well were counted, and these counts were converted to percentages by comparing the TUNEL-positive counts to the total number of cell nuclei as determined by DAPI counterstaining.

2.10.   Immunocytochemistry

Immunocytochemistry was performed in order to detect and localize NRF2 proteins in control and treated cells according to the previous protocol (Sohel et al., 2017) with some modifications. Briefly, 2×105 viable cells were seeded in each well of a 24-well culture plate and after the treatments cells from each category were washed three times in warm DPBS and then cells were fixed in 4% paraformaldehyde at 4°C for overnight, washed 3 times with DPBS, permeabilized using 0.2% TritonX-100 (Sigma-Aldrich) in PBS at room temperature for 1 h, and washed with 3 times in DPBS for 5 min. After blocking with 3% normal donkey serum in DPBS for 1 h at room temperature, cells were incubated with specific primary antibody against NRF2 (1:100 dilution, SC-722, Santa Cruz Biotechnology, Dallas, Texas) for overnight at 4°C. In the next day, cells were washed twice with 0.05% Tween20 (P9416, Sigma) in DPBS and incubated further with FITC conjugated donkey anti-rabbit secondary antibody (1:200 dilution, SC-2090, Santa Cruz Biotechnology, Dallas, Texas) for 1 h at 37°C in dark. After washing twice with DPBS, cells were incubated with 3 ng/mL 4´,6´-diamidino-2-phenylindole (DAPI; Vector Laboratories) in DPBS to stain the nucleus for 5 min in dark and fluorescence microscopy was performed using Nikon Eclipse Ti-S microscope (Nikon Instruments Inc., Tokyo, Japan) using green and blue-fluorescence filter and images were acquired by NIS Elements software.

2.11.   Real time quantitative PCR for candidate genes

The resulting cDNA samples were then used to investigate the expression of target genes were GAPDH was considered as a reference in Roche Light cycler 480 real-time PCR machine (Roche Life Science, Penzberg, Germany). The stability of GAPDH expression was tested among the samples (data not shown). The qRT-PCR reaction was set up by adding 10 µl 1× Power SYBR Green I (Bio-Rad, Hercules, CA) master mix, 0.3 µM of forward and reverse gene specific primers, 7.4 µl deionized water and 2 µl first-strand cDNA template. The thermal

cycling conditions were 3 min at 95°C followed by 40 cycles of 15 seconds at 95°C and 1 min at 60°C. Comparative CT ($2^{-\Delta\Delta CT}$) method was employed to analyze the relative expression of each mRNA. Using a sequence specific primers, a total of 7 genes namely NRF2, KEAP1, Caspase 3 (CASP3), superoxide dismutase-1 (SOD1), peroxiredoxin1 (PRDX1), thioredoxin-1 (TXN1) and catalase (CAT) were examined for their expression in GCs. The primers were designed using primer3web version 4.0.4 (http://bioinfo.ut.ee/primer3/) and the sequences are listed in Supplementary Table 1.

Table 2.1: List of primers for quantitative RT-PCR

Gene symbol	Accession number	Primer Sequences	Annealing temperature (°C)	Product size (BP)
GAPDH	NM_001034034	F 5´- CCAGGGCTGCTTTTAATTCT R 5´- ATGGCCTTTCCATTGATGAC	56	247
NFE2L2	NM_001011678	F 5´- CCCAGTCTTCACTGCTCCTC R 5´- TCAGCCAGCTTGTCATTTTG	55	165
KEAP1	NM_001101142.1	F 5´- TCACCAGGGAAGGATCTACG R 5´- AGCGGCTCAACAGGTACAGT	55	199
CAT	NM_001035386.1	F 5´- TGGGACCCAACTATCTCCAG R 5´- AAGTGGGTCCTGTGTTCCAG	51	178
TXN1	NM_173968.3	F 5´- AGCTGCCAAGATGGTGAAAC R 5´- ACTCTGCAGCAACATCCTGA	55	215
PRDX1	NM_174431.1	F 5´- TGGATCAACACACCCAAGAA R 5´- GTCTCAGCGTCTCATCCACA	55	217
SOD1	NM_174615	F 5´- AGAGGCATGTTGGAGACCTG R 5´- CAGCGTTGCCAGTCTTTGTA	53	189

2.12. miRNA profiling and expression analysis

The expression profiles of miRNAs in the cells of control and oxidatively stressed groups were performed using ready-to-use Human miRNA PCR Panel containing 83 mature miRNAs specific to apoptosis (MISH-114Z, Qiagen) following the manufacturers' instruction. The real-time PCR was run on a Roche Light cycler 480 real-time PCR machine (Roche Life Science, Penzberg, Germany) using the following thermal-cycling parameters: 95°C for 15 min, 40 cycles of 94°C for 15 s, 55°C for 30 s, 70°C for 30 s followed by a melting curve analysis. The raw data from PCR were analyzed by web-based PCR array data analysis software provided by SAbioscience (http://pcrdataanalysis.sabiosciences.com/pcr/arrayanalysis.php). The raw miRNA data were normalized using the normalizer miRNAs present in the PCR plate. To minimize the potential noise introduced by measurements below the detection threshold, miRNAs with Ct value greater than 35 in all groups were considered as undetected.

2.13. Target prediction and pathway analysis

One miRNA can target several protein coding miRNAs, similarly, a single protein coding mRNA can be targeted by several miRNAs. Therefore, it is important to identify the biological relevance of the differentially regulated miRNAs. To predict the potential targets of differentially regulated miRNAs, we used miRDB and TargetScans web based miRNA target prediction algorithms. Predicted target genes were screened and the duplicate values were removed from the list. The screened genes were then uploaded to DAVID Bioinformatics Resource (http://david.abcc.ncifcrf.gov/) server for Annotation, Visualization, and Integrated Discovery to identify the pathway distribution. These pathways were presented according to the Kyoto Encyclopedia of Genes and Genomes (KEGG) database (http://www.genome.jp/kegg/).

2.14.   Statistical analysis

A minimum of three biological replicates was performed in each experiment. Statistical differences between treatment group means (quantitative variables) were analyzed by one-way ANOVA followed by multiple pairwise comparisons (Tukey test, $\alpha=0.05$). For statistical analyses and graphs, SPSS version 20.0 and Excel 2016 were used. Data are expressed as mean $\pm$ SEM of three biological replicates. Differences were considered as significant at $p<0.05$.

3. Results

3.1. Viability of GCs in different concentrations of SFN

Despite its beneficial role against oxidative stress, higher concentrations of SFN are reported to have detrimental effects on survival and function of different cell types. Therefore, we investigated the effect of a wide range of concentrations of SFN (0, 1, 2, 5, 10, 15, 20, 40, and 80 µM) on GCs to identify the concentration where the cells started to face additional stress and drop their viability significantly and 0.05% DMSO-treated cells were considered as control. The effects of various concentrations of SFN on the viability of GCs were determined by trypan blue exclusion test, and results are shown in Fig. 3.1A. Although no significant difference was found up to 10 µM concentration, consistently reduced viability was observed at higher concentrations. For instance, 98-97% viability was observed at 1-2 µM concentrations, whereas the viability of GCs was ~90% at 10 µM concentration. On the other hand, survival ability of GCs reduced significantly upon a 24-h exposure at ≥15 µM concentrations of SFN and lowest viability was observed at the highest concentration (80 µM) of SFN (Fig. 3.1A).
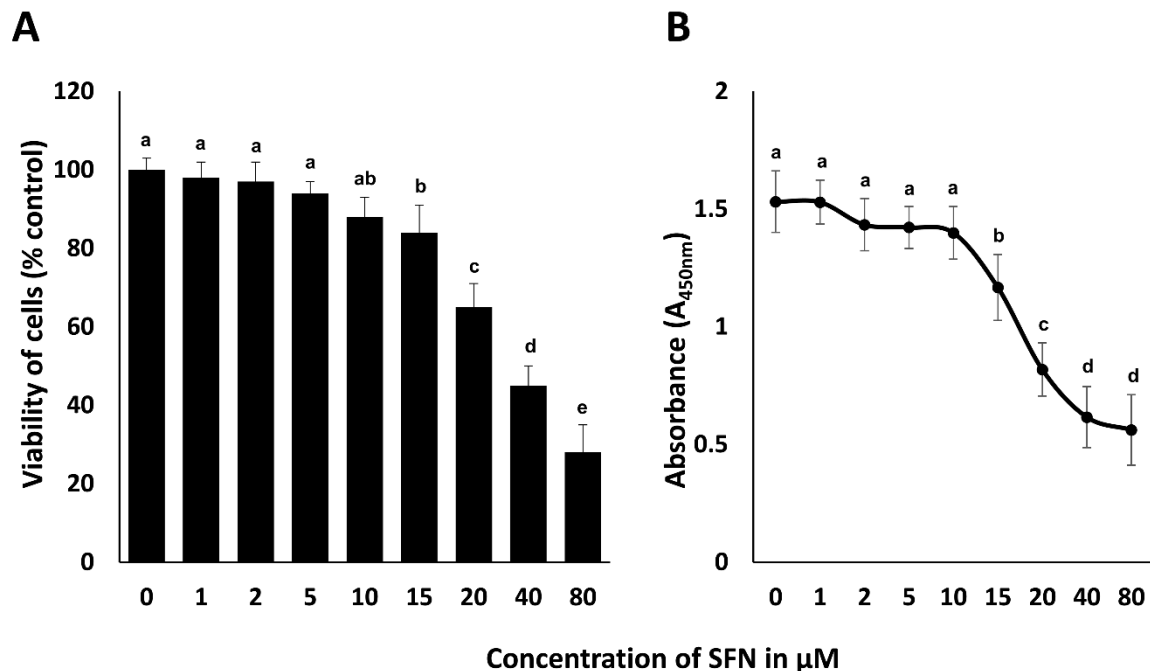

Figure 3.1: Viability and cytotoxic effects of different concentration of SFN in GCs. After an exposure with SFN (ranging from 0 to 80 µM) for 24 h, cells were subjected to trypan blue dye exclusion test for cell viability (A) or WST-1 test for cytotoxic effect in different concentrations (B). Different superscript letters (a, b, c, d, e) denote a significant difference between groups, such that groups not sharing a similar letter are significantly different from each other ($p < 0.05$).

According to the viability test, it is clear that SFN caused a dose dependent loss of cell viability in GCs which, perhaps, indicating a higher level of cytotoxicity on GCs at higher concentrations. Therefore, we sought to determine the cytotoxic effects of indicated concentrations of SFN on GCs using WST-1 reagent and the results are presented in Fig. 1B. The results revealed that SFN-induced cytotoxicity was also dose dependent and followed a similar pattern like viability results. For instance, low doses of SFN <5 µM had no significant cytotoxic effect, whereas medium concentrations (~10 µM) had very little cytotoxic effects and higher concentrations >15 µM were found to be extremely cytotoxic to GCs (Fig. 3.1B). It is important to note that, both viability and cytotoxicity test suggested that lower concentrations of SFN had no cytotoxic effect, while higher concentrations are highly cytotoxic and had detrimental impacts on cell viability.

3.2. SFN enhance the expression of NRF2 and attenuates the expression of KEAP1

Based on phenotypic observations, out of eight concentrations, three different concentrations were chosen for further investigations, i.e. 2, 10, and 20 µM representing low, medium, and high doses of SFN, respectively. We first investigated the expression level of NRF2 and KEAP1 mRNAs under different concentration of SFN in order to have an idea whether the 'Nrf2-ARE pathway' is activated or not. Analysis of qRT-PCR data revealed that no significant changes in the expression of NRF2 were observed in cells treated with 2 µM SFN, while a significant increase in the expression of NRF2 was observed in 10 and 20 µM SFN treated groups (Fig. 3.2A). Although no significant difference in the expression of NRF2 was observed between 10 and 20 µM concentrations, higher expression trend was found in the cells treated with 20 µM concentration. Expression of KEAP1 decreased in SFN treated GCs compared to untreated control (Fig. 3.2B). Compared to control, no significant difference in KEAP1 expression was observed in cells treated with 2 µM SFN. However, significantly lower KEAP1 expression was observed in 10 and 20 µM SFN concentrations (Fig. 3.2B).
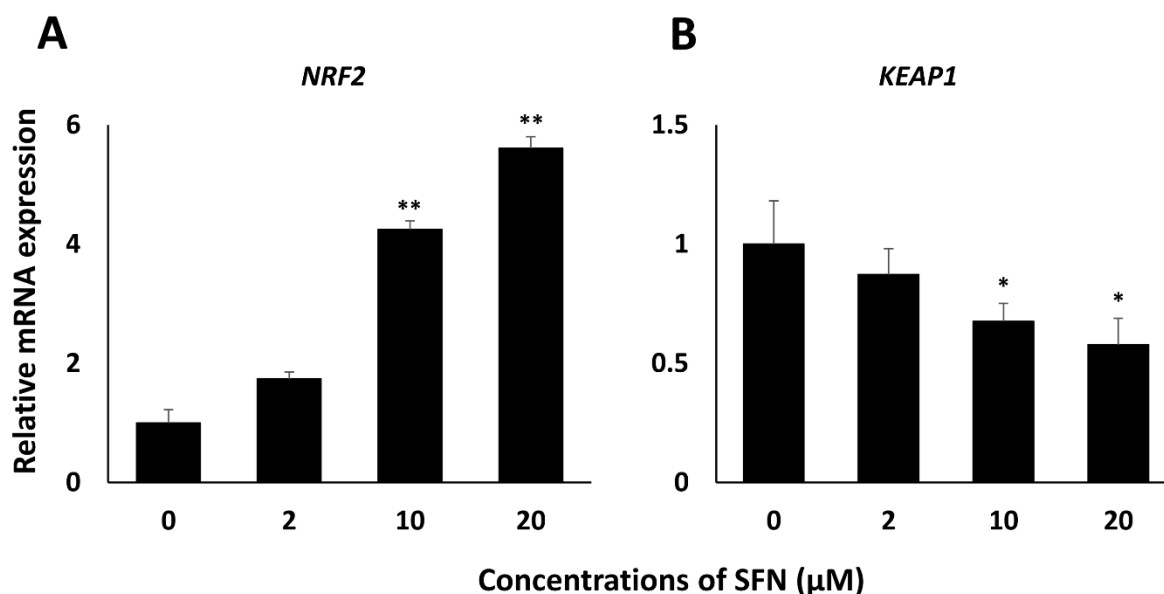
Figure 3.2: Relative abundance of NRF2 and KEAP1. To elucidate the Nrf2 pathway activation in response to the different concentration of SFN (2, 10, and 20 µM), we employed real-time qPCR to investigate the relative expression of (A) NRF2 and (B) KEAP1. The statistically significance of the effect of different treatments on gene expression is marked with asterisks, where * = $p < 0.05$, ** = $p < 0.01$). Data are presented as means ± SD of three biological replicates.

3.3. Expression of ARE genes downstream to Nrf2 pathway

Next, we investigated the expression level of selected antioxidant genes downstream of NRF2 activation, namely PRDX1, CAT, TXN1, and SOD1 using qRT-PCR. Interestingly, almost similar expression patterns were observed for all candidate genes (Fig. 3.3A-D). For instance, no significant difference was observed in any of the antioxidant genes at 2 µM concentration. However, expression of all genes significantly increased in GCs treated with 10 or 20 µM SFN concentrations compared to control (0.05% DMSO) (Fig. 3.3A-D). Although expression of PRDX1 significantly increased at 20 µM compared to 10 µM (Fig. 3.3A), no significant differences were observed in other genes at these concentrations (Fig. 3.3B-D).
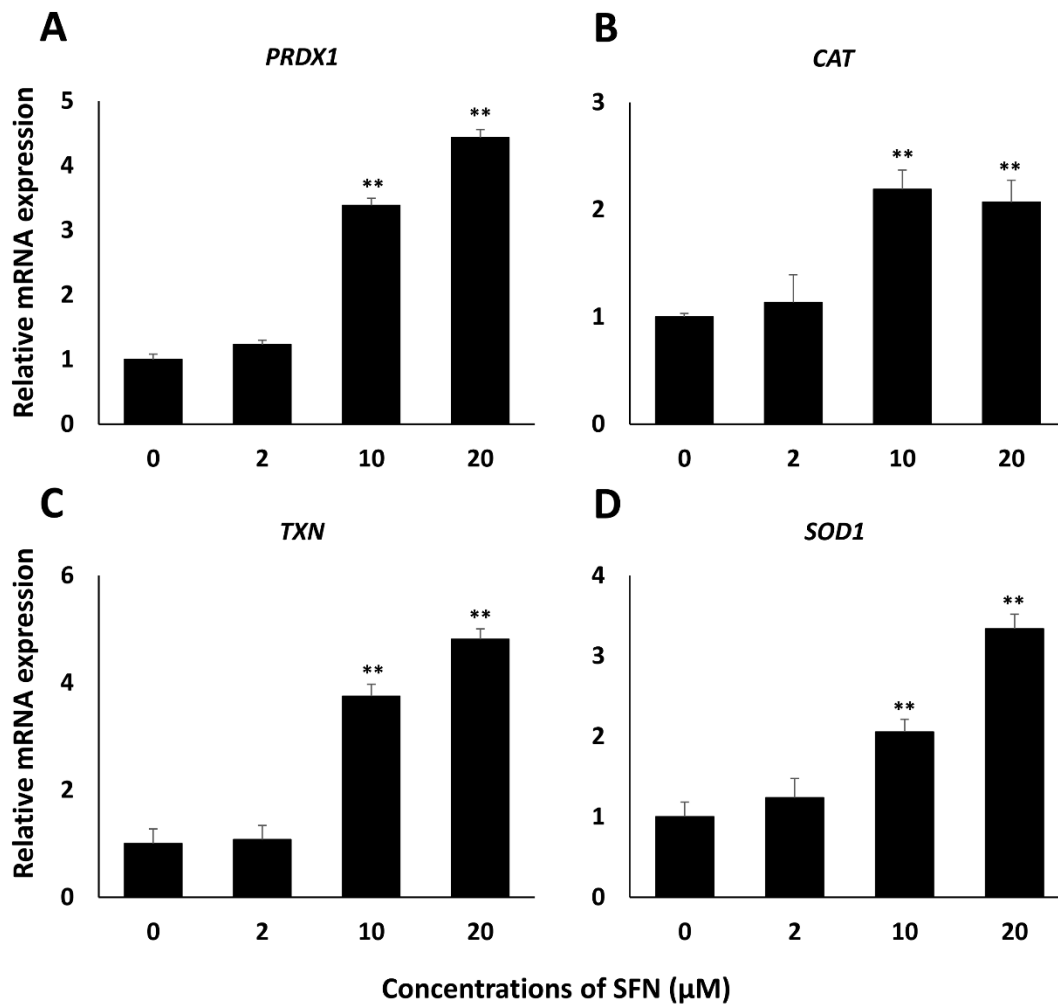
Figure 3.3: Expression of ARE genes downstream to NRF2 activation. Upon exposure to a different concentration of SFN (0, 2, 10, and 20 μM), the relative abundance of down-stream genes PRDX1 (A), CAT (B), TXN (C), and SOD1 (D) at mRNA level was measured by real time qPCR. Different asterisks represent statistically significant differences where ** = p < 0.01. Data are presented as means ± SD of three biological replicates.

3.4. High concentration of SFN increases the expression of genes associated with apoptosis in GCs

In order to investigate whether a high concentration of SFN induces cell death through the apoptotic pathway, we sought to investigate the expression of BAX and CASP3 in GCs treated with different concentrations of SFN. As shown in Fig. 3.4A, there was no significant difference in the expression level of BAX in 2 μM and 10 μM concentration compared to control. A significant increase (3 fold) in the expression level of BAX was observed in the cells exposed

to 20 µM SFN. Similar to BAX, no significant difference was observed in the expression level of CASP3 in 2 µM SFN and slightly increased expression (~2 fold) were observed in 10 µM concentration; however, significantly higher expression (~5 fold) was found in 20 µM SFN (Fig. 3.4B).
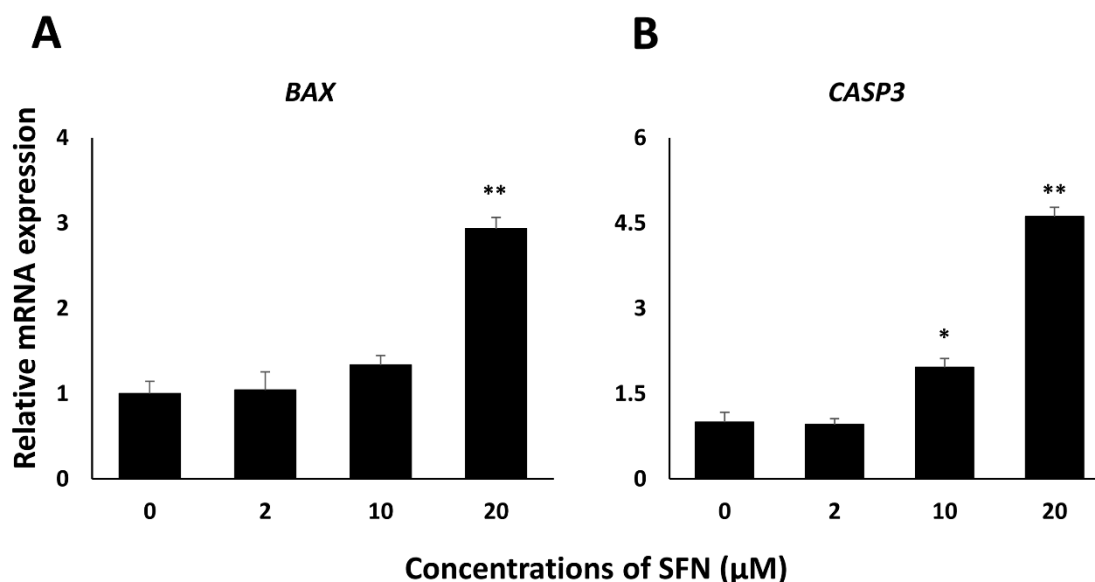

Figure 3.4: Expression of BAX and CASP3 genes. In order to identify whether SFN induces the expression of genes related to apoptosis, GCs were exposed to different concentration of SFN (0, 2, 10, and 20 µM) and relative abundance of BAX (A) and CASP3 (B) were measured by real time qPCR at mRNA level. Statistically significant effects of different treatments on gene expression is marked with asterisks where * = $p < 0.05$ and ** = $p < 0.01$. Data are presented as means ± SD of three biological replicates.

3.5. High concentration of SFN leads to higher GC apoptosis

To further verify the role of SFN in inducing cellular apoptosis, GCs were grown in 96-well plate and treated according to the experimental plan. The results of in situ detection of fragmented DNA by TUNEL assay in GCs cultured with different concentrations of SFN are presented in Fig. 3.5. Only 0.5% TUNEL-positive cells were detected in untreated control GCs, while 2.3% and 3.3% TUNEL-positive cells were present in 2 µM and 10 µM SFN treated GCs, respectively (Fig. 3.5). Significantly higher number of apoptotic cells (32%) were detected after 24 h of incubation with 20 µM SFN (Fig. 3.5).
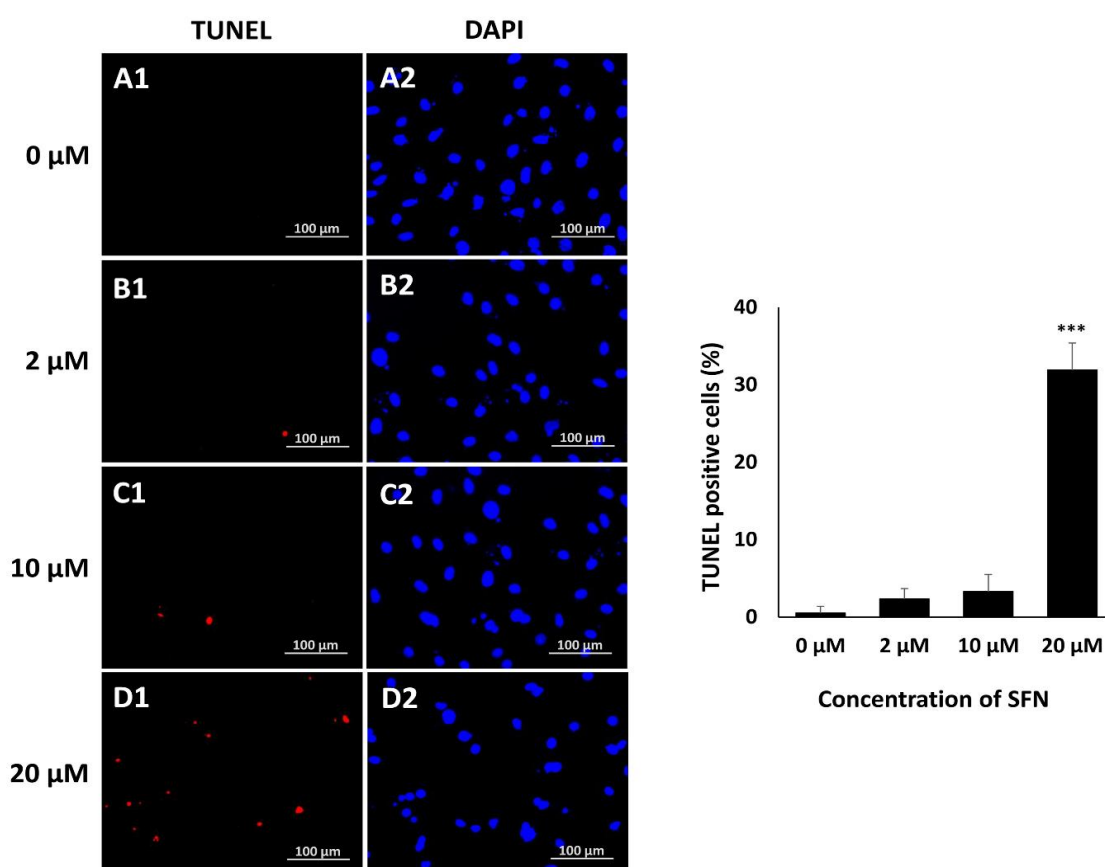
Figure 3.5: In situ detection of fragmented DNA by TUNEL assay and simultaneous nuclear staining with DAPI. 1×10^4 viable GCs were seeded in each well of a 96-well plate (flat bottom, tissue culture treated) and grown up to 50-60% confluence and different concentration of SFN was added according to the experimental plan. The results of TUNEL assay showed that 20 µM SFN significantly increased the number of TUNEL-positive apoptotic nuclei after 24 h of incubation, whereas very less TUNEL positive cells were observed in untreated control, 2 µM, and 10 µM SFN concentrations (Fig. 5 A1-D1). Left panel: representative micrographs of double staining of TUNEL (red fluorescent) and DAPI (blue, counter staining), scale bar 100 µm; right panel: quantitative data analysis of TUNEL-positive cells where *** = p < 0.001; data are presented as mean ± SD of three biological replicates.

3.6.   SFN causes higher accumulation of ROS and lipid droplets at higher concentrations

We next investigated the accumulation of ROS in order to understand the SFN induced loss of cell viability is indeed due to excessive production of intracellular ROS. GCs were incubated

with different concentrations of SFN and after 24h incubation cells were subjected to ROS sensitive fluorescent dye H2DCFDA. As shown in Fig. 3.6A-B, exposure to SFN generates ROS in GCs in a concentration dependent manner. No differences were observed between 0 and 2 µM SFN treatment and there was a slight increase in ROS accumulation in 10 µM concentration. A sharp increase in ROS accumulation was observed in GCs treated with 20 µM SFN (Fig. 3.6A-B).

An excessive level of ROS can induce activation of SREBP which eventually enhance lipid synthesis and formation of lipid droplets in cells. Therefore, we next investigated the accumulation of lipid droplets in SFN treated cells. Interestingly, compared to control a decreased intensity of Oil Red O stain was observed in cells treated with 2 µM SFN indicating lower lipid droplet accumulation (Fig. 3.6C). While accumulation of lipid droplets slightly increased in 10 µM SFN which is somewhat similar to control, excessive lipid droplet accumulation was observed in cells exposed to 20 µM SFN (Fig. 3.6C).
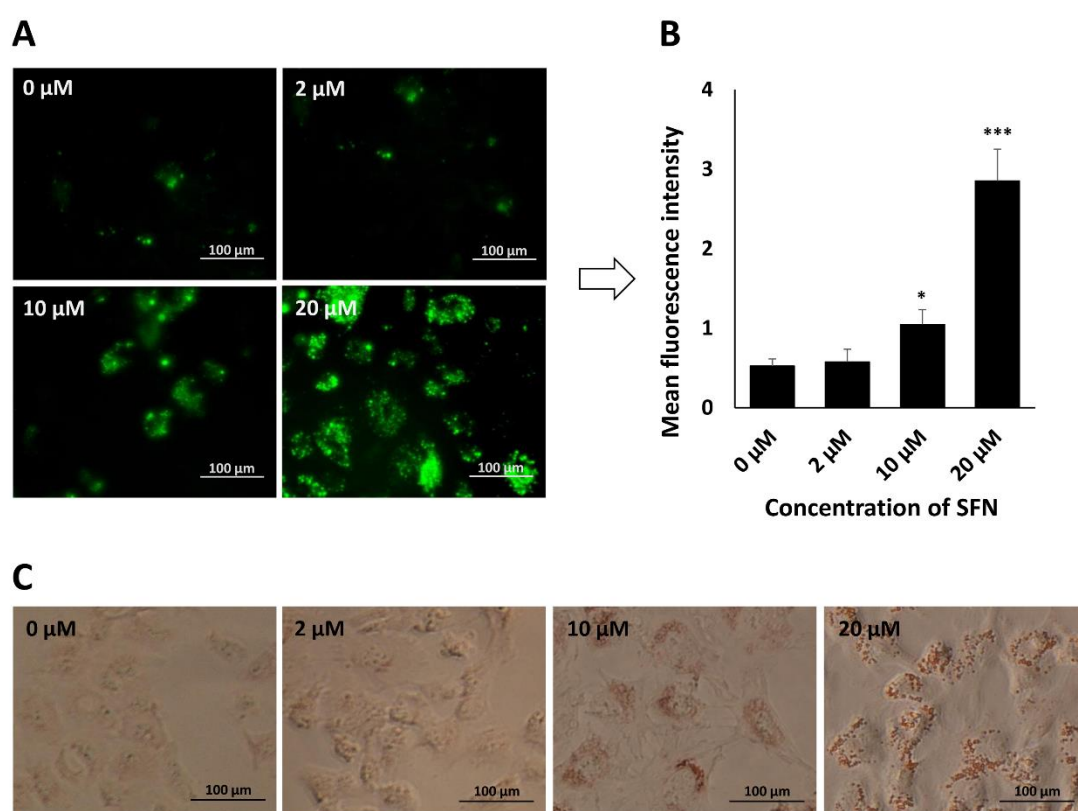

Figure 3.6: ROS and lipid droplet accumulation in GCs after treatment with different concentration of SFN. GCs were exposed to SFN (0, 2, 10, and 20 µM) for 24 h, (A) washed and loaded with H2DCFDA (5 µM for 30 min) and visualized under a fluorescent microscope, scale

bar 100 µm (B) Mean fluorescence intensity was quantified by ImageJ software from five nonoverlapping fields per well, experiments were performed in triplicates; * = p < 0.05 and *** = p < 0.001; data are presented as mean ± SD. (C) Following treatment, GCs were loaded with Oil Red O stain working solution (for 40 min), washed several times and visualized with an inverted microscope. Scale bars, 50 µm.

3.7.   Higher concentration of SFN results in low mitochondrial activity in GCs

Although electron transport chain of mitochondria is the major source of intracellular ROS, mitochondria itself is one of the primary targets of ROS induced damage and dysfunction. In order to assess the effects higher SFN induced excessive ROS on mitochondrial function, mitochondrial activity was determined in cells exposed to different concentration of SFN.
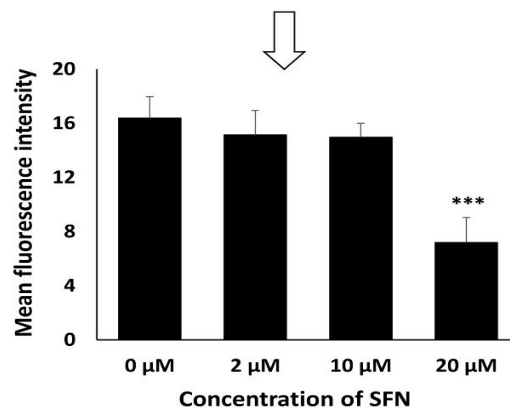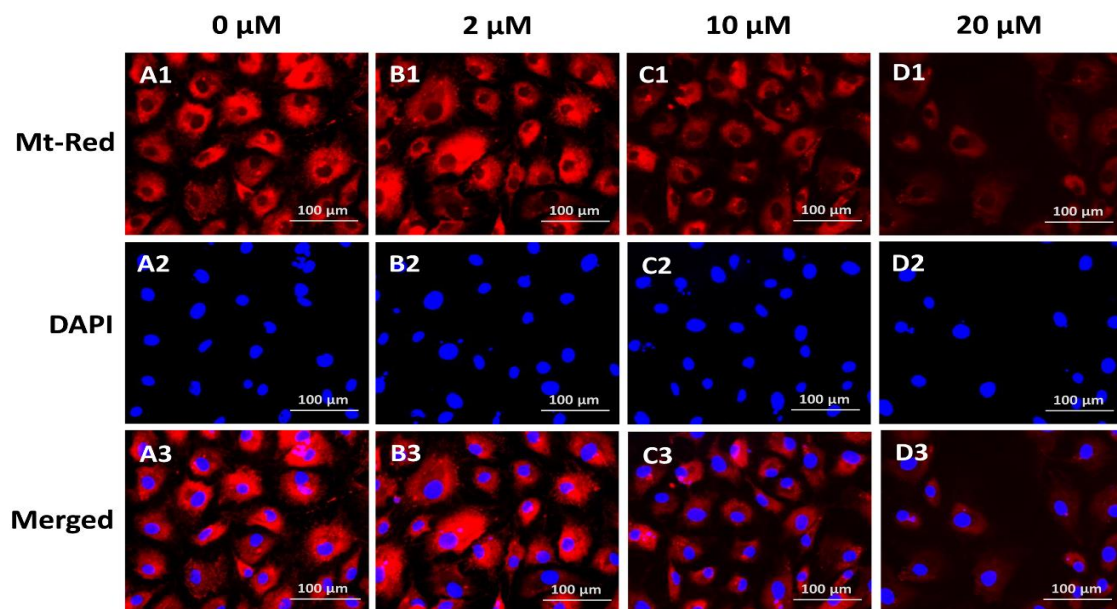
Figure 3.7: Mitochondrial activity in GCs at different concentrations of SFN. GCs were treated according to the experimental plan and 100 nM Mito Tracker red dye was added and incubated for 45 min. Images were acquired with a fluorescence microscope using a red filter. Higher panel: labels A1-D1 show active mitochondria in red, while A2-D2 show nuclear staining with DAPI in blue color and A3-D3 show merged image of active mitochondria and nucleus staining. Scale bars, 50 µm. Lower panel: mean fluorescence intensity of five nonoverlapping fields per well was quantified using ImageJ software; experiments were performed in triplicates; *** = p < 0.001; data are presented as mean ± SD.

Similar mitochondrial activity like untreated control was observed in cells exposed to 2 and 10 µM SFN, as evidenced by similar fluorescence intensity detected by fluorescence microscopy (Fig. 3.7 B-C). Notably, lower activity of mitochondria was observed in cells exposed to 20 µM SFN indicating mitochondrial dysfunction under high concentration of SFN (Fig. 3.7D).

3.8 Characterization of oxidative stress in GCs

To investigate whether the expressions of GC miRNAs are changed due to OS, GCs were grown and stimulated with 75 µM H2O2 for 24 h to develop a cell model of oxidative stress. GCs in both control and OS group were examined after 24 h of culture period using an inverted microscope for the morphological changes. The morphometric observation confirms that the cells in OS group showed typical signs of stress characterized by shrinkage in size, lower number of live cells and a higher number of dead cells compared to control (Fig. 1A). The results of cell viability, using trypan blue exclusion test, showed that there was a significant (p < 0.001) loss cell viability in OS stressed group compared to untreated control (Fig. 1B) which further indicates the presence of OS. In addition, the results of cell viability assay strengthen the findings of morphometric observation and viability test as it also showed a lower number of viable cells, perhaps, due to the existence of OS in H2O2 treated cells indicated by significantly lower absorbance value (Fig. 1C).

Following our observation of the morphologic changes and the decrease in the cell survival due to H2O2 stimulation, next, we sought to investigate differences in the generation of ROS molecules in the control and H2O2 treated groups as excessive production of ROS is the hallmark of OS. Administration of 75 µM H2O2 for 24h resulted higher accumulation of ROS

in cells which is evidenced by the higher fluorescence intensity (Fig. 1D) and histogram analysis of fluorescence intensity across the image revealed that mean fluorescence intensity increased significantly ($p < 0.001$) in OS group compared to untreated control (Fig. 1F).

Under OS condition, the Nrf2 translocate from cytoplasm to nucleus in order to start the transcription of a battery of antioxidant enzymes which eventually scavenges the excessive ROS. Keeping this fact in mind, next we investigate the location of Nrf2 in both untreated control and OS group using immunocytochemistry technique. The results showed that Nrf2 was predominantly located in the cytoplasm in the cells of the untreated control group, whereas almost all the Nrf2 were in the nucleus (Fig. 1E).
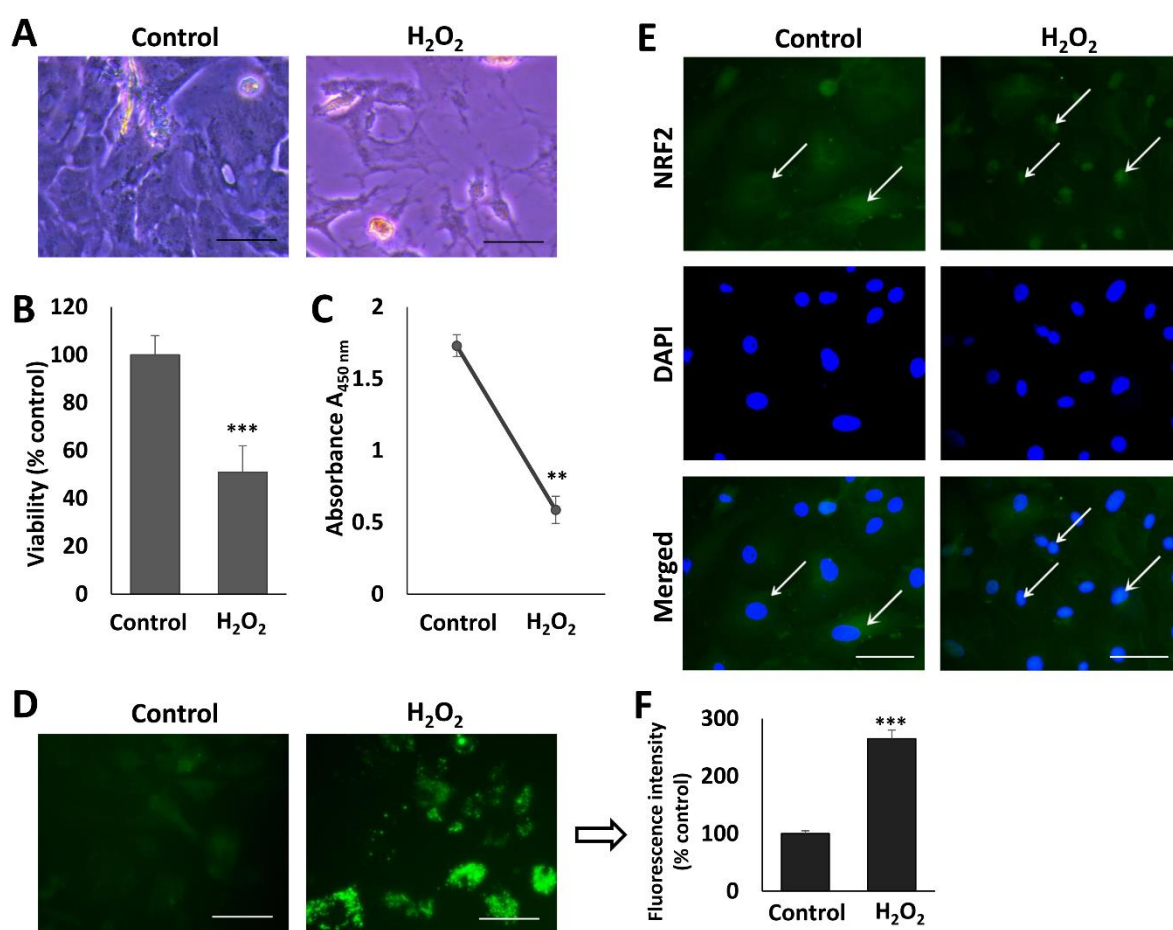

Fig. 3.8: Characterization of oxidative stress in GCs. A) cell culture photos after 24 h of culture. B) The viability of cells under oxidative stress determined by trypan blue exclusion test. C) Analysis of cytotoxicity assay using WHT-1 assay kit. D, F) Accumulation of ROS molecules E) In situ localization of NRF2 using immunocytochemistry.

3.9. Number of detected miRNAs

To understand whether miRNAs modulated by OS plays a role in apoptosis, the expression of miRNAs in GCs was quantified by ready to use 96-well PCR plates (Qiagen, Hilden) containing 86 mature human miRNAs mostly related to apoptosis (either proapoptotic or antiapoptotic) and 10 endogenous controls. The presence of miRNAs was determined based crossing point (Cp) value and the % of detection within the replicates. miRNAs were considered as detected when their Cp values were less than 35 and present in at least 68% of the samples. The Cp value was set based on our previous experiences in detecting miRNAs in the qPCR array based platform (Noferesti et al., 2015; Sohel et al., 2013).
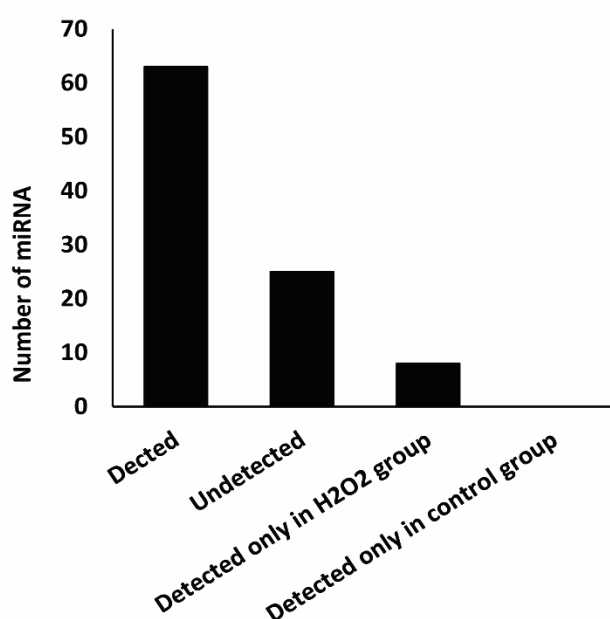
Fig. 3.9: Number of detected miRNAs. On an average, a total of 63 miRNAs were detected, 26 miRNAs were undetected and 8 miRNAs were detected only in the cells of the oxidative stress group.

Off the 86 miRNAs investigated, a total of 58 miRNAs were detected in the cells of the control group, while 66 miRNAs were detected in the cells of OS group. There are at least 8 miRNAs which were detected only in the cells of OS group. These miRNAs were either undetected or Cp values were more than 35 in the cells of the control group.

3.10. Differential expression of miRNAs in GCs exposed to OS

We next tested our hypothesis whether OS modulates the expression of miRNAs in GCs. Expression of miRNAs in the cells of OS and Control group was analyzed using web-based miScript miRNA PCR Array Data analysis software provided SABiosiences. Of the detected 66 miRNAs, a total of 27 miRNAs were differentially regulated, in which 17 miRNAs were upregulated and 10 miRNAs were downregulated with a range of 2 – 18-fold. Among the upregulated miRNAs, miR-365b-3p showed highest fold change regulation, whereas miR-210-3p showed highest fold change regulation among downregulated miRNAs (Table 3.1).

Table 3.1. List of miRNAs that are differentially regulated due to oxidative stress

Name of the microRNA	Fold change (Control vs. Treatment)	P value
miR-365b-3p	18.15	0.011439
miR-26b-5p	14.69	0.001867
let-7c-5p	6.67	0.003948
miR-143-3p	5.75	0.000003
miR-29a-3p	4.49	0.007341
miR-204-5p	4.02	0.005066
miR-16-5p	4	0.020813
miR-206	3.61	0.035981
miR-409-3p	3.42	0.020641
miR-149-3p	3.33	0.000002
miR-128-3p	3.06	0.009743
miR-25-3p	2.83	0.003128
miR-181a-5p	2.8	0.015152
miR-708-5p	2.67	0.015844
miR-125a-5p	2.34	0.000002
miR-153-3p	2.23	0.000042
miR-512-5p	2.08	0.000071
miR-141-3p	-2.18	0.012844
miR-92a-3p	-2.29	0.011760
miR-186-3p	-2.95	0.050975
miR-125b-5p	-3.27	0.013494
miR-106b-5p	-3.32	0.031496
miR-221-3p	-5.47	0.012695
miR-98-5p	-6.01	0.000263
miR-378a-3p	-7.27	0.004742

| miR-145-5p | -9.43 | 0.002325 |
| miR-210-3p | -9.91 | 0.009260 |

3.11. Cluster of miRNAs affected by oxidative stress

Clustered miRNAs are a group of miRNAs those are situated within 10,000 kb of distance on the same chromosome. A typical cluster contains two or three miRNAs, although large clusters are not uncommon. Of the differentially regulated miRNAs with a fold change more than 2, we found that 45% miRNAs are in different clusters while remaining miRNAs are acted as

Cluster # 1: miR-143 ~ 145
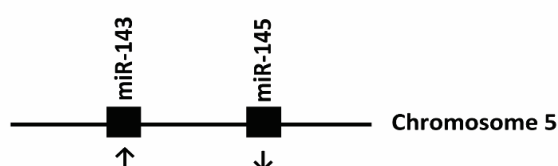
Cluster # 2: miR-25 ~ 106b
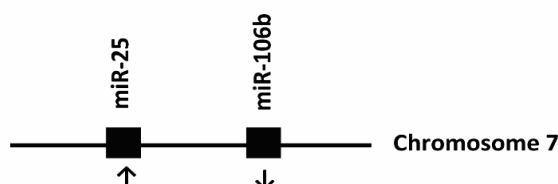
Fig. 3.10. Complete clusters of miRNAs affected by oxidative insult.

individual miRNA. Two complete miRNA clusters, namely miR-143 ~ 145 and miR-25 ~ 106b, were affected by the oxidative stress treatment (Fig. 3.10). Both of the clusters contain two miRNA genes. One of the clusters was found on chromosome 5, while another cluster was found on chromosome 7. Interestingly, in both of the clusters, one miRNA showed upregulation and other miRNA showed down regulation. It is a general assertion that miRNAs in a cluster may have a similar expression pattern. In our experiment, we found different expression pattern within the miRNA members of both clusters. It is may be due to the nature of the miRNAs, for instance, both miR-145 and miR-106b show either pro- or anti-apoptotic characteristics depending on the pathophysiological condition.

3.12. Number of genes targeted by oxidative stress modulated miRNAs

A single miRNA can target multiple genes, while a gene can also be targeted by several miRNAs. Therefore, we generated lists genes predicted to be targeted by all differentially regulated miRNAs. All the individual gene list for both upregulated and downregulated miRNAs were merged and subsequently, duplicate values were removed from the merged list. A total of 9432 and 4491 genes were predicted to be targeted by the upregulated and downregulated miRNAs, respectively. When duplicate values were removed, 6210 and 3575 genes were left in the gene list of upregulated and downregulated miRNA, respectively. Detail information about the number of target genes predicted to be targeted by individual miRNA in both up and downregulated miRNAs are listed in Table 3.2 and Table 3.4.

Table 3.2: List of a total number of target genes and the name of top 10 genes predicted by upregulated miRNAs.

Name of the microRNA	Number of genes	Official symbol of top 10 genes
miR-365b-3p	278	SGK1, HHIP, USP33, NR1D2, DLAT, UBAC2, UBP1, TIAM2, ZC3HAV1, UNC5D
miR-26b-5p	518	SLC2A13, SLC7A11, FAM98A, SLC45A4, ZDHHC6, PITPNC1, STRADB, RNF6, ZNF608, USP9X
let-7c-5p	435	SMARCAD1, FAM178A, LIN28B, GATM, LRIG3, GNPTAB, BZW1, ZNF322, ADAMTS8, C8orf58
miR-143-3p	375	GXYLT1, VASH1, ITM2B, ATP10A, IGFBP5, MSI2, ATP6V1A, MOGS, DENND1B, DIP2B
miR-29a-3p	632	BRWD3, COL3A1, ERCC6, DGKH, ATAD2B, FBN1, NFIA, TET3, NAV3, ROBO1
miR-204-5p	599	C9orf72, RAB22A, AP1S2, ANKRD13A, EBF2, ACSL4, ZNF423, PTPRD, SASS6, SPRED1
miR-16-5p	1089	ZFHX4, SYNJ1, SLC9A6, IPO7, CDCA4, NUP50, PAPPA, LUZP1, SLC13A3, UNC80
miR-206	417	PTPLAD1, GLCCI1, LPPR4, ZMAT3, TPPP, CDK14, ANKRD29, EIF4E, NRP1, C2orf69
miR-409-3p	258	KIAA2022, YTHDF3, NXPH1, SLC35A3, KLF15, OXR1, CPSF6, RAB10, ZDHHC20
miR-149-3p	1461	NFIX, C20orf96, SSBP3, HCFC1, SPRY4, SOX13, NACC1, PVRL1, AR, RAB5B
miR-128-3p	625	PAIP2, SZRD1, NFX1, POGLUT1, EFR3A, BAG2, AK2, SEC22A, LBH, TRIL
miR-25-3p	496	DNAJB9, CD69, SYNJ1, FBXW7, SLC12A5, EFR3A, MAP2K4, USP28, KIAA1109, KIAA1432
miR-181a-5p	887	C2CD5, FIGN, S1PR1, PDE5A, MTMR12, TBC1D1, TNPO1, PROX1, OSBPL3, MICU3
miR-708-5p	277	GPM6A, PAPPA, FAM107A, TNS3, TEF, HOXA1, KIAA0355, FOXJ3, JPH1, EN2
miR-125a-5p	479	IRF4, LACTB, OSBPL9, ZSWIM6, ENPEP, HIF1AN, GCNT1, SLC39A9, SMEK1, SEMA4D
miR-153-3p	365	YIPF2, SLC4A4, OSBPL6, EBF2, NFE2L2, PLCB1, NAV2, RAI14, DMD, UTRN
miR-512-5p	242	BAZ2A, ATRX, PHF6, HLTF, CENPL, TBL1XR1, PRR14L, HSPA12A, DDX6, SRPK2

Table 3.3: List of a total number of target genes and the name of top 10 genes predicted by downregulated miRNAs.

Name of the microRNA	Number of genes	Official symbol of top 10 genes
miR-210-3p	39	FGFRL1, ISCU, RRP1B, DENND6A, IGF2, ZNF462, DHX58, KMT2D, CORO2B, ACVR1B
miR-145-5p	495	ABCE1, MPZL2, DAB2, KCNA4, ABHD17C, AP1G1, YTHDF2, SPSB4, ATP8A1, SEMA3A
miR-378a-3p	169	NR2C2, KIAA1522, TMEM245, SLC7A6, MPP3, RAB10, SERINC1, NKX3-1, FLT1, ELAC1
miR-98-5p	437	SMARCAD1, LIN28B, FAM178A, GNPTAB, LRIG3, GATM, ADAMTS8, DNA2, ADRB2, BZW1
miR-221-3p	316	GABRA1, PANK3, TCF12, CDKN1B, HECTD2, RFX7, TMCC1, FNDC3A, ARF4, C3orf70
miR-106b-5p	855	PTPN4, ARID4B, EPHA4, PKD2, PDCD1LG2, SLC40A1, FBXL5, ZNF800, ADARB1, ZNFX1
miR-125b-5p	476	IRF4, ZSWIM6, ENPEP, LACTB, OSBPL9, GCNT1, HIF1AN, IER3IP1, SEMA4D, SLC39A9
miR-186-3p	551	MAML2, MYCBP, HLCS, RAB11FIP1, KDM2A, HMBOX1, LIN54, TMEM181, UBE2Q1, BCL6
miR-92a-3p	496	SYNJ1, DNAJB9, EFR3A, SLC12A5, USP28, FBXW7, CD69, APPL1, MOAP1, MAP2K4
miR-141-3p	759	DUSP3, TMEM170B, ZBTB34, DCP2, ATP8A1, MYBL1, ZEB2, TRHDE, HS2ST1, ELAVL2

3.13. Enriched pathways to be affected by the differentially regulated miRNAs

To identify the potential pathways to be affected by the genes targeted by the differentially expressed miRNAs, we used DAVID Bioinformatics Resource. To overcome the limitation of DAVID Bioinformatics Resource (limited processing ability: 3,000 genes), only top 100 genes were considered for each miRNA for further bioinformatics analysis. Accordingly, after screening of the long list of genes, 1447 and 720 genes were identified as potential targets of up- and down-regulated miRNAs, respectively.

Table 3.4: List of top 10 enriched pathways that are predicted to be targeted by the upregulated miRNAs

Pathway name	miRNAs involved	P value
Platelet activation	miR-25-3p, miR-29a-3p, miR-365b-3p,	2.48E-07
Focal adhesion	miR-16-5p, miR-25-3p, miR-26b-5p, miR-29a-3p, miR-143-3p, miR-149-3p,	5.29E-07
mTOR signaling pathway	miR-16-5p, miR-26b-5p, miR-29a-3p, miR-149-3p, miR-181a-3p,	6.64E-06
FoxO signaling pathway	miR-16-5p, miR-25-3p, miR-29a-3p, miR-153-3p, miR-181a-3p, miR-204-5p, miR-365b-3p, miR-512-5p,	1.31E-05
Prostate cancer	miR-29a-3p, miR-149-3p, miR-181a-3p, miR-365b-3p,	1.52E-05

Neurotrophin signaling pathway	miR-16-5p, miR-29a-3p, miR-143-3p, miR-149-3p, miR-181a-3p, miR-204-5p, miR-708-5p	2.61E-05
Axon guidance	miR-26b-5p, miR-149-3p, miR-153-3p, miR-204-5p, miR-206, miR-708-5p	3.04E-05
Signaling pathways regulating pluripotency of stem cells	miR-16-5p, miR-29a-3p, miR-149-3p, miR-708-5p	3.37E-05
PI3K-Akt signaling pathway	miR-16-5p, miR-25-3p, miR-29a-3p, miR-143-3p, miR-149-3p, miR-153-3p, miR-181a-3p, miR-365b-3p,	4.22E-05
Proteoglycans in cancer	miR-16-5p, miR-25-3p, miR-149-3p, miR-153-3p, miR-181a-3p,	4.41E-05

As shown in Table 3.4, several pathways including platelet activation, focal adhesion, FoxO signaling pathway neurotrophin signaling pathway, axon guidance, and PI3K-Akt signaling pathway have been shown to be affected by upregulated miRNAs. Most of the pathways are known to be involved in different cellular processes and development. Off the top 10 pathways, FoxO signaling pathway and PI3K-Akt signaling pathway were targeted by maximum miRNAs, i.e. both pathways are targeted by 8 miRNAs.

Table 3.5: List of top 10 enriched pathways that are predicted to be targeted by the upregulated miRNAs

Pathway name	miRNAs involved	P value
Proteoglycans in cancer	miR-92a-3p, miR-106b-5p, miR-141-3p, miR-221-3p,	6.88E-07
MAPK signaling pathway	miR-106b-5p, miR-141-3p, miR-221-3p,	1.47E-06
Endocytosis	miR-106b-5p, miR-141-3p, miR-378a-3p	1.17E-05
Rap1 signaling pathway	miR-141-3p, miR-221-3p,	3.83E-05
Thyroid hormone signaling pathway	miR-106b-5p,	4.21E-05
Pathways in cancer	miR-92a-3p, miR-106b-5p, miR-141-3p, miR-221-3p, miR-378a-3p	5.12E-05
Chronic myeloid leukemia	miR-106b-5p, miR-141-3p,	5.39E-05
FoxO signaling pathway	miR-92a-3p, miR-106b-5p, miR-141-3p,	7.76E-05
Hepatitis B	miR-92a-3p, miR-106b-5p, miR-141-3p, , miR-221-3p,	1.12E-04
Prolactin signaling pathway	miR-106b-5p, miR-141-3p, miR-221-3p,	1.61E-04

On the other hand, a number of pathways including proteoglycans in cancer, MAPK signaling pathway, neurotrophin transduction, signal transmission, cancer development were affected by the downregulated miRNAs. Interestingly, FoxO signaling pathway was targeted by both up

and downregulated miRNAs. It is a general assertion that miRNA target prediction may contain both false negative and positive results, therefore, to understand the potential function of these deregulated miRNAs can only be established using functional experiments.

4. Discussion and Conclusion

One of the major factors in oxidative stress induced cell injury or death is the production of excessive amount of ROS and cell's inability to produce sufficient antioxidant enzymes to scavenge those excessive ROS (Poljsak et al., 2013). On the course of evolution, the cell has developed an inherent defense mechanism in response to different stress or stimuli- the activation of the Nrf2 signaling pathway to produce a wide range of antioxidant enzymes (Espinosa-Diez et al., 2015). Our results clearly demonstrated that medium concentration of SFN is able to activate the Nrf2-ARE pathway in bovine GCs as evidenced by higher expression of NRF2 and lower expression of KEAP1 genes. In addition, expression of selected antioxidant genes downstream to NRF2 activation was also found to be highly expressed upon exposure to the medium concentration of SFN. It is important to note that the viability and cell proliferation were not affected significantly by the medium concentration of SFN. Interestingly, low concentration of SFN had no significant effects on either activating Nrf2 signaling pathway or influencing cell viability. On the other hand, a high concentration of SFN exhibited adverse effects on GCs. Although it induced a significant increase in the expression of NRF2 and its downstream antioxidant genes, it also enhanced the expression of genes related to apoptosis. Furthermore, a high concentration of SFN increased the generation of ROS which leads to mitochondrial dysfunction and apoptosis in GCs.

SFN has been found to be unfavorable for the proliferation and survival of many types of cancer cells (Kensler et al., 2013; Zhang and Tang, 2007) including ovarian cancer cells (Chaudhuri et al., 2007; Chuang et al., 2007), while in other somatic cells certain concentrations of SFN induce the protection against oxidative and other environmental stresses (Nair et al., 2007). Several studies have shown using cell culture, in carcinogen-induced and genetic animal cancer model, and xenograft model of cancer that the potential of using SFN as a therapeutic agent in cancer treatment (Lenzi et al., 2014). In addition, cell culture and animal studies have provided convincing evidence for the use of SFN to induce the phase II detoxifying and antioxidant enzymes in different kind of somatic cells (Boddupalli et al., 2012). It is highly likely that, in near future, SFN will be used as a drug to combat against cancer or to maintain cellular homeostasis against oxidative stress in human. However, in either case, the concentration of SFN carries utmost importance as different concentration induces different pathways (Boddupalli et al., 2012). Interestingly, the concentration dependent impacts of SFN on GCs have not been investigated yet. By employing a wide range of concentrations (1e80 mM) of SFN, we showed that 2e10 mM SFN had no detrimental effects in terms of survival and

proliferation of GCs, whereas high concentrations (20 mM) exhibited cytotoxic effects (Fig. 1) characterized by a lower number of viable cells. In addition, particular apoptotic morphological characteristics including irregular cell shape, shrinkage of the cell wall, and more floating cells in the culture media were detected after the treatment with higher concentrations (data not shown). Similar to our findings, Lee and Lee reported a concentration dependent loss of viability in Human Bronchial Epithelial BEAS-2B Cells that exposed to SFN for 24 h (Lee and Lee, 2011). Perhaps, low concentration of SFN activates the genes related to cell survival pathway, while high concentration induces the expression of genes involved in antiproliferative and apoptotic pathways. Therefore, it is of interest to investigate the effect of low and high concentration of SFN on GCs in activating genes related to both survival and apoptotic pathway.

NRF2 transcription factor regulates and coordinates more than 200 genes in mammals largely known to be involved in enhancing endogenous antioxidant defense system and survival capability of cells (Petri et al., 2012). The endogenous antioxidant defense system consists of a wide range of phase II detoxification enzymes such as glutathione transferase, SOD, catalase (CAT), and heme oxygenase (HO-1). Expression of these antioxidant enzymes is regulated by ARE promoter sequence which is modulated by NRF2 transcription factor (Ma, 2013; Petri et al., 2012). In our study, we found that the expression of NRF2 increased significantly in GCs exposed to 10 and 20 mM SFN, while the expression of KEAP1 decreased significantly under similar conditions. SFN has been proven to be an efficient modifier of multiple KEAP1 domains in the NRF2-KEAP1 interactions (Hong et al., 2005; Hu et al., 2011); consequently, NRF2 released from the interactions and be able to translocate into the nucleus where it can modulate the transcription of Phase II antioxidant enzymes by interacting with ARE. Therefore, it is highly likely that the higher expression of NRF2 and Phase II antioxidant enzymes in our experiment is due to the disruption of the NRF2-KEAP1 interactions caused by SFN treatments. Our findings are consistent with the previous reports demonstrated that low concentration of SFN enhances the activity of NRF2 and induces the transcription of phase II antioxidant enzymes in many cell types (Jacob et al., 2013).

One of the crucial elements in the behavior of mammalian cells is the activation of apoptotic pathways under unfavorable environmental conditions (Jacobson et al., 1997). In this process, a series of enzymes participated in a tightly coordinated manner which is regulated by specific genes known as pro-apoptotic or apoptotic genes such as CASP3, BAX, BAK, BID, BAD, BIM, BIK, and BLK (Elmore, 2007). The products of these genes have special significance as

they can determine the fate of cells. In our experiment, we found that there was a significant increase in the expression of both BAX and CASP3 in GCs treated with 20 mM SFN which may suggest the activation of apoptotic pathway in the presence of high concentration of SFN which was further supported by results of TUNEL assay. BAX can be found predominantly in the cytosol; however, on induction of apoptosis, it could partially be translocated to the mitochondria (Narita et al., 1998; Wolter et al., 1997). This shift induces the mitochondrial permeability transition pore to open and facilitates the release of cytochrome c which eventually activates the caspase cascade (Narita et al., 1998).

Oxidative stress induced cell death is believed to be associated with higher accumulation of intracellular ROS (Ryter et al., 2007). Interestingly, it has been shown that SFN induced apoptosis and cell death is also initiated by excessive generation of intracellular ROS (Lee and Lee, 2011; Singh et al., 2005). Our results revealed that there was a higher accumulation of ROS at high concentration as indicated by increased fluorescence activity. On the other hand, a slight increase in the accumulation of ROS was observed in GCs exposed 2 and 10 mM SFN. Intracellular ROS generation induced by SFN plays an important role in the induction of apoptosis through cell cycle arrest in many cancer cells. Interestingly, under similar concentrations, other somatic cells are not affected as they can scavenge elevated level of ROS through activating antioxidant defense mechanism and show resistance to cell cycle arrest and apoptosis (Nair et al., 2007; Sestili and Fimognari, 2015). In our study, probably ROS has generated such a high rate, at high concentration, that cells were unable to scavenge by producing sufficient antioxidant enzymes resulting cell cycle arrest and cell death. Elevated ROS level can induce lipogenesis via activating SREBPs in cells under culture condition resulting higher accumulation of lipid droplets (Lee et al., 2015). Therefore, it is not surprising that we found an elevated accumulation of lipid droplets in GCs exposed to 20 mM SFN. However, in this study, we did not check the underlying mechanism of lipid accumulation in GCs exposed to high concentration of SFN which warrant further experimental attention.

Although mitochondria are the major site of ROS generation, it is also highly susceptible to the oxidative damage caused by ROS, particularly mitochondrial DNA and electron transport chain. In active mitochondria, mitochondrial antioxidant defense enzymes such as glutathione peroxidase and manganese SOD scavenge ROS produced during ATP synthesis (Dröse and Brandt, 2012). However, under stress conditions, excessive generation of ROS can impair the capacity of this defense system, resulting in mitochondrial damage. Importantly, damaged mitochondria can produce even more ROS due to impaired electron transportation chain

(Maharjan et al., 2014). Subsequently, excessive ROS can decrease the mitochondrial membrane potential and facilitate the release of cytochrome c and apoptosis inducing factors which eventually activate the pro-apoptotic cascade resulting in cell death through apoptosis. Mito Tracker probes are able to differentiate an active mitochondrion from a damaged one since it can defuse the plasma membrane and accumulate in active mitochondria. In the present study, we found less mitochondrial activity in GCs treated with high concentration of SFN, as evidenced by less fluorescence, perhaps indicating loss of mitochondrial membrane integrity caused by ROS and induction of apoptotic cascade.

miRNAs are small non-coding RNA species of 18-22 nt long and are known to be the master regulator of gene expression (Hossain et al., 2012). Since their discovery, miRNAs are the widely studied because of their potential involvement in various developmental and biological process and disease (Soifer et al., 2007). The association of miRNAs with diseases have been reported in the context of potential involvement in diseases or developmental processes via their expression pattern or function. Several studies have been conducted focusing on the involvement of miRNAs during the development of various disorder due to stress, particularly oxidative stress. For instance, oxidative stress induced modulation of miRNA regulation has been reported in mouse primary hippocampal neurons, in vascular disease, in Parkinson disease, and in so many other cases. In addition, the role of miRNAs in granulosa cell function has been reported in several species including human, cattle, swine, and mouse. However, a functional link between miRNA expression and oxidative stress in granulosa cells remains to be investigated. Here in this project, we investigated the expression of several miRNAs related to apoptosis in primary culture of granulosa cells.

The miRNA expression analysis confirms that there was a massive deregulation in the expression of miRNAs in GCs due to oxidative stress. We found, 27 miRNAs were differentially regulated, of these 17 miRNAs were upregulated and remaining 10 miRNAs were downregulated. The differential expression of several miRNAs confirms that oxidative stress modulates the expression and function of different miRNAs in GCs. Among the upregulated miRNAs, miR-365b-3p, miR-26b-5p, let-7c-5p, miR-143-3p and miR-29a-3p showed higher fold change regulation. All of these miRNAs are known to be involved in the process of cellular apoptosis. On the other hand, miR-221-3p, miR-98-5p, miR-378a-3p, miR-145-5p, and miR-210-3p showed higher fold change regulation among the downregulated miRNAs. These miRNAs are known to be involved in different cellular processes and cellular defense system.

From the miRNA expression study, it is clear that oxidative stress results in apoptosis by modulating the expression of several miRNAs known to be involved in the cellular apoptosis.

It was considered that miRNAs conducted themselves as key regulators in maintaining transcriptome homeostasis (Ezzie et al., 2012). To analyze the possible biological effects of deregulated miRNAs after H2O2 stimulation, we predicted the target mRNAs of changed miRNAs and performed an enrichment analysis of multiple miRNA target genes by KEGG. The results showed that H2O2-induced miRNAs mainly took part in the MAPK pathway, Neurotrophin signaling pathway, Axon guidance, Steroid biosynthesis and Insulin signaling pathway. Among them, the MAPK pathway was one of the most significant candidate pathways to be affected by H2O2-induced up-regulated miRNAs (Son et al., 2011). This signaling cascade is involved in a number of cell functions, including cell development, differentiation, synaptic plasticity, and learning. In recent years, it has been reported that MAPK is essential for LTP formation in the rodent hippocampus (Gehart et al., 2010). Thus, we hypothesized that H2O2-induced miRNAs deregulation of MAPK cascade may partly contribute to the loss of function in GCs.

In summary, our results showed that low dose of SFN is able to activate an antioxidative response in GCs which is evidenced by higher expression of Nrf2 and its downstream antioxidant enzymes at the transcription level. Although we found a slight increase of ROS level at low concentrations, it did not affect the activity and integrity of mitochondria. Perhaps, low levels of ROS are generated in response to low doses of SFN and cellular antioxidants are able to scavenge them. Instead of damaging the cellular macromolecule, it may boost up the antioxidant defense system in GCs. On the other hand, a high concentration of SFN is extremely cytotoxic to GCs as we found lower cell viability, high ROS and lipid droplet accumulation and, low mitochondrial activity. These results provoke us to conclude that depending on concentrations SFN has both antioxidative and apoptosis effects on GCs. In addition, expression of several miRNAs was differentially regulated in the cells of oxidative stress group. Further analysis confirms that these miRNAs are mostly related to the regulation of cellular apoptosis. Taken together, our study confirms that the alteration of the expression of miRNAs and mRNA is associated with the survival or apoptosis pathways in the GCs under oxidative stress.

5- References

Afonso-Grunz, F., Müller, S., 2015. Principles of miRNA–mRNA interactions: beyond sequence complementarity. Cell. Mol. Life Sci. 72, 3127–3141. doi:10.1007/s00018-015-1922-2

Alfadda, A.A., Sallam, R.M., 2012. Reactive Oxygen Species in Health and Disease. J. Biomed. Biotechnol. 2012, 1–14. doi:10.1155/2012/936486

Baley, J., Li, J., 2012. MicroRNAs and ovarian function. J. Ovarian Res. 5, 1–7. doi:10.1186/1757-2215-5-8

Boddupalli, S., Mein, J.R., Lakkanna, S., James, D.R., 2012. Induction of Phase 2 Antioxidant Enzymes by Broccoli Sulforaphane: Perspectives in Maintaining the Antioxidant Activity of Vitamins A, C, and E. Front. Genet. 3, 7. doi:10.3389/fgene.2012.00007

Brieger, K., Schiavone, S., Miller, J., Krause, K., 2012. Reactive oxygen species: from health to disease. Swiss Med. Wkly. doi:10.4414/smw.2012.13659

Chaudhuri, D., Orsulic, S., Ashok, B.T., 2007. Antiproliferative activity of sulforaphane in Akt-overexpressing ovarian cancer cells. Mol. Cancer Ther. 6, 334–45. doi:10.1158/1535-7163.MCT-06-0404

Chuang, L.T., Moqattash, S.T., Gretz, H.F., Nezhat, F., Rahaman, J., Chiao, J.-W., 2007. Sulforaphane induces growth arrest and apoptosis in human ovarian cancer cells. Acta Obstet. Gynecol. Scand. 86, 1263–1268. doi:10.1080/00016340701552459

Donadeu, F.X., Schauer, S.N., Sontakke, S.D., 2012. Involvement of miRNAs in ovarian follicular and luteal development. J. Endocrinol. 215, 323–34. doi:10.1530/JOE-12-0252

Dou, Y.-D., Zhao, H., Huang, T., Zhao, S.-G., Liu, X.-M., Yu, X.-C., Ma, Z.-X., Zhang, Y.-C., Liu, T., Gao, X., Li, L., Lu, G., Chan, W.-Y., Gao, F., Liu, H.-B., Chen, Z.-J., 2016. STMN1 Promotes Progesterone Production Via StAR Up-regulation in Mouse Granulosa Cells. Sci. Rep. 6, 26691. doi:10.1038/srep26691

Dröse, S., Brandt, U., 2012. Molecular mechanisms of superoxide production by the mitochondrial respiratory chain. Adv. Exp. Med. Biol. 748, 145–69. doi:10.1007/978-1-4614-3573-0_6

Elmore, S., 2007. Apoptosis: a review of programmed cell death. Toxicol. Pathol. 35, 495–516. doi:10.1080/01926230701320337

Espinosa-Diez, C., Miguel, V., Mennerich, D., Kietzmann, T., Sánchez-Pérez, P., Cadenas, S., Lamas, S., 2015. Antioxidant responses and cellular adjustments to oxidative stress. Redox Biol. 6, 183–97. doi:10.1016/j.redox.2015.07.008

Ezzie, M.E., Crawford, M., Cho, J.-H., Orellana, R., Zhang, S., Gelinas, R., Batte, K., Yu, L., Nuovo, G., Galas, D., Diaz, P., Wang, K., Nana-Sinkam, S.P., 2012. Gene expression networks in COPD: microRNA and mRNA regulation. Thorax 67, 122–131. doi:10.1136/thoraxjnl-2011-200089

Gehart, H., Kumpf, S., Ittner, A., Ricci, R., 2010. MAPK signalling in cellular metabolism: stress or wellness? EMBO Rep. 11, 834–40. doi:10.1038/embor.2010.160

Guerrero-Beltrán, C.E., Calderón-Oliver, M., Pedraza-Chaverri, J., Chirino, Y.I., 2012. Protective effect of sulforaphane against oxidative stress: recent advances. Exp. Toxicol. Pathol. 64, 503–8. doi:10.1016/j.etp.2010.11.005

Hong, F., Freeman, M.L., Liebler, D.C., 2005. Identification of sensor cysteines in human Keap1 modified by the cancer chemopreventive agent sulforaphane. Chem. Res. Toxicol. 18, 1917–26. doi:10.1021/tx0502138

Hossain, M.M., Sohel, M.M.H., Schellander, K., Tesfaye, D., 2012. Characterization and importance of microRNAs in mammalian gonadal functions. Cell Tissue Res. 349, 679–90. doi:10.1007/s00441-012-1469-6

Hu, C., Eggler, A.L., Mesecar, A.D., van Breemen, R.B., 2011. Modification of keap1 cysteine residues by sulforaphane. Chem. Res. Toxicol. 24, 515–21. doi:10.1021/tx100389r

Itoh, K., Chiba, T., Takahashi, S., Ishii, T., Igarashi, K., Katoh, Y., Oyake, T., Hayashi, N., Satoh, K., Hatayama, I., Yamamoto, M., Nabeshima, Y., 1997. An Nrf2/Small Maf Heterodimer Mediates the Induction of Phase II Detoxifying Enzyme Genes through Antioxidant Response Elements. Biochem. Biophys. Res. Commun. 236, 313–322. doi:10.1006/bbrc.1997.6943

Jabbour, H.N., Sales, K.J., Catalano, R.D., Norman, J.E., 2009. Inflammatory pathways in female reproductive health and disease. Reproduction 138, 903–19. doi:10.1530/REP-09-0247

Jacob, K.D., Noren Hooten, N., Trzeciak, A.R., Evans, M.K., 2013. Markers of oxidant stress that are clinically relevant in aging and age-related disease. Mech. Ageing Dev. 134, 139–57. doi:10.1016/j.mad.2013.02.008

Jacobson, M.D., Weil, M., Raff, M.C., 1997. Programmed Cell Death in Animal Development. Cell 88, 347–354. doi:10.1016/S0092-8674(00)81873-5

Johnson, A.L., Solovieva, E.V., Bridgham, J.T., 2002. Relationship Between Steroidogenic Acute Regulatory Protein Expression and Progesterone Production in Hen Granulosa Cells During Follicle Development. Biol. Reprod. 67, 1313–1320. doi:10.1095/biolreprod67.4.1313

Kang, K.W., Lee, S.J., Kim, S.G., 2005. Molecular mechanism of nrf2 activation by oxidative stress. Antioxid. Redox Signal. 7, 1664–73. doi:10.1089/ars.2005.7.1664

Kensler, T.W., Egner, P.A., Agyeman, A.S., Visvanathan, K., Groopman, J.D., Chen, J.-G., Chen, T.-Y., Fahey, J.W., Talalay, P., 2013. Keap1-nrf2 signaling: a target for cancer prevention by sulforaphane. Top. Curr. Chem. 329, 163–77. doi:10.1007/128_2012_339

Khan, H.A., Zhao, Y., Wang, L., Li, Q., Du, Y.-A., Dan, Y., Huo, L.-J., 2015. Identification of miRNAs during mouse postnatal ovarian development and superovulation. J. Ovarian Res. 8, 1–11. doi:10.1186/s13048-015-0170-2

Laurent, L.C., 2008. MicroRNAs in embryonic stem cells and early embryonic development. J. Cell. Mol. Med. 12, 2181–8. doi:10.1111/j.1582-4934.2008.00513.x

Lee, J., Homma, T., Kurahashi, T., Kang, E.S., Fujii, J., 2015. Oxidative stress triggers lipid droplet accumulation in primary cultured hepatocytes by activating fatty acid synthesis, Biochemical and Biophysical Research Communications. doi:10.1016/j.bbrc.2015.06.121

Lee, Y.-J., Lee, S.-H., 2011. Sulforaphane induces antioxidative and antiproliferative responses by generating reactive oxygen species in human bronchial epithelial BEAS-2B cells. J. Korean Med. Sci. 26, 1474–82. doi:10.3346/jkms.2011.26.11.1474

Lenzi, M., Fimognari, C., Hrelia, P., 2014. Sulforaphane as a Promising Molecule for Fighting Cancer, in: Cancer Treatment and Research. pp. 207–223. doi:10.1007/978-3-642-38007-5_12

Li, C., Chen, C., Chen, L., Chen, S., Li, H., Zhao, Y., Rao, J., Zhou, X., 2016. BDNF-induced expansion of cumulus-oocyte complexes in pigs was mediated by microRNA-205. Theriogenology 85, 1476–1482. doi:10.1016/j.theriogenology.2016.01.004

Lim, J., Ortiz, L., Nakamura, B.N., Hoang, Y.D., Banuelos, J., Flores, V.N., Chan, J.Y., Luderer, U., 2015. Effects of deletion of the transcription factor Nrf2 and benzo [a]pyrene treatment on ovarian follicles and ovarian surface epithelial cells in mice. Reprod. Toxicol.

58, 24–32. doi:10.1016/j.reprotox.2015.07.080

Loukides, J.A., Loy, R.A., Edwards, R., Honig, J., Visintin, I, Polan, M.L., 1990. Human Follicular Fluids Contain Tissue Macrophages*. J. Clin. Endocrinol. Metab. 71, 1363–1367. doi:10.1210/jcem-71-5-1363

Ma, Q., 2013. Role of nrf2 in oxidative stress and toxicity. Annu. Rev. Pharmacol. Toxicol. 53, 401–26. doi:10.1146/annurev-pharmtox-011112-140320

Maharjan, S., Oku, M., Tsuda, M., Hoseki, J., Sakai, Y., 2014. Mitochondrial impairment triggers cytosolic oxidative stress and cell death following proteasome inhibition. Sci. Rep. 4, 1–11. doi:10.1038/srep05896

Michiels, C., Raes, M., Toussaint, O., Remacle, J., 1994. Importance of Se-glutathione peroxidase, catalase, and Cu/Zn-SOD for cell survival against oxidative stress. Free Radic. Biol. Med. 17, 235–48.

Mukherjee, S., Lekli, I., Ray, D., Gangopadhyay, H., Raychaudhuri, U., Das, D.K., 2010. Comparison of the protective effects of steamed and cooked broccolis on ischaemia-reperfusion-induced cardiac injury. Br. J. Nutr. 103, 815–23. doi:10.1017/S0007114509992492

Nair, S., Li, W., Kong, A.-N.T., 2007. Natural dietary anti-cancer chemopreventive compounds: redox-mediated differential signaling mechanisms in cytoprotection of normal cells versus cytotoxicity in tumor cells. Acta Pharmacol. Sin. 28, 459–472. doi:10.1111/j.1745-7254.2007.00549.x

Narita, M., Shimizu, S., Ito, T., Chittenden, T., Lutz, R.J., Matsuda, H., Tsujimoto, Y., 1998. Bax interacts with the permeability transition pore to induce permeability transition and cytochrome c release in isolated mitochondria. Proc. Natl. Acad. Sci. U. S. A. 95, 14681–6.

Pan, B., Toms, D., Shen, W., Li, J., 2015. MicroRNA-378 regulates oocyte maturation via the suppression of aromatase in porcine cumulus cells. Am. J. Physiol. Endocrinol. Metab. 308, E525-34. doi:10.1152/ajpendo.00480.2014

Peng, Y., Croce, C.M., 2016. The role of MicroRNAs in human cancer. Signal Transduct. Target. Ther. 2016, 1–9. doi:10.1038/sigtrans.2015.4

Petri, S., Korner, S., Kiaei, M., 2012. Nrf2/ARE Signaling Pathway: Key Mediator in Oxidative Stress and Potential Therapeutic Target in ALS. Neurol. Res. Int. 2012, 1–7.

doi:10.1155/2012/878030

Poljsak, B., Suput, D., Milisav, I., 2013. Achieving the Balance between ROS and Antioxidants: When to Use the Synthetic Antioxidants. Oxid. Med. Cell. Longev. 2013, 1–11. doi:10.1155/2013/956792

Rahal, A., Kumar, A., Singh, V., Yadav, B., Tiwari, R., Chakraborty, S., Dhama, K., 2014. Oxidative Stress, Prooxidants, and Antioxidants: The Interplay. Biomed Res. Int. 2014, 1–19. doi:10.1155/2014/761264

Romaine, S.P.R., Tomaszewski, M., Condorelli, G., Samani, N.J., 2015. MicroRNAs in cardiovascular disease: an introduction for clinicians. Heart 101, 921–8. doi:10.1136/heartjnl-2013-305402

Ryter, S.W., Kim, H.P., Hoetzel, A., Park, J.W., Nakahira, K., Wang, X., Choi, A.M.K., 2007. Mechanisms of Cell Death in Oxidative Stress. Antioxid. Redox Signal. 9, 49–89. doi:10.1089/ars.2007.9.49

Sestili, P., Fimognari, C., 2015. Cytotoxic and Antitumor Activity of Sulforaphane: The Role of Reactive Oxygen Species. Biomed Res. Int. 2015, 1–9. doi:10.1155/2015/402386

Shkolnik, K., Tadmor, A., Ben-Dor, S., Nevo, N., Galiani, D., Dekel, N., 2011. Reactive oxygen species are indispensable in ovulation. Proc. Natl. Acad. Sci. U. S. A. 108, 1462–7. doi:10.1073/pnas.1017213108

Sies, H., 1997. Oxidative stress: oxidants and antioxidants. Exp. Physiol. 82, 291–295. doi:10.1113/expphysiol.1997.sp004024

Simpson, K., Wonnacott, A., Fraser, D.J., Bowen, T., 2016. MicroRNAs in Diabetic Nephropathy: From Biomarkers to Therapy. Curr. Diab. Rep. 16, 35. doi:10.1007/s11892-016-0724-8

Singh, S. V, Srivastava, S.K., Choi, S., Lew, K.L., Antosiewicz, J., Xiao, D., Zeng, Y., Watkins, S.C., Johnson, C.S., Trump, D.L., Lee, Y.J., Xiao, H., Herman-Antosiewicz, A., 2005. Sulforaphane-induced cell death in human prostate cancer cells is initiated by reactive oxygen species. J. Biol. Chem. 280, 19911–24. doi:10.1074/jbc.M412443200

Sohel, M.H., Cinar, M.U., Kalibar, M., Arslan, K., Sariozkan, S., Akyuz, B., Konca, Y., 2016. Appropriate concentration of Hydrogen Peroxide and Sulforaphane for granulosa cells to study oxidative stress in vitro. J. Biotechnol. 231, S24. doi:10.1016/j.jbiotec.2016.05.104

Sohel, M.M.H., 2016. Extracellular/Circulating MicroRNAs: Release Mechanisms, Functions and Challenges. Achiev. Life Sci. 10, 175–186. doi:10.1016/j.als.2016.11.007

Sohel, M.M.H., Cinar, M.U., 2015. Advancement in Molecular Genetics to understand the molecular reproduction of Livestock – follicular development. Res. Agric. Livest. Fish. 1, 47–60. doi:10.3329/ralf.v1i1.22355

Sohel, M.M.H., Hoelker, M., Noferesti, S.S., Salilew-Wondim, D., Tholen, E., Looft, C., Rings, F., Uddin, M.J., Spencer, T.E., Schellander, K., Tesfaye, D., 2013. Exosomal and non-exosomal transport of extra-cellular microRNAs in follicular fluid: Implications for bovine oocyte developmental competence. PLoS One 8. doi:10.1371/journal.pone.0078505

Sohel, M.M.H., Konca, Y., Akyuz, B., Arslan, K., Sariozkan, S., Cinar, M.U., 2017. Concentration dependent antioxidative and apoptotic effects of sulforaphane on bovine granulosa cells in vitro. Theriogenology 97, 17–26. doi:10.1016/j.theriogenology.2017.04.015

Soifer, H.S., Rossi, J.J., Saetrom, P., 2007. MicroRNAs in disease and potential therapeutic applications. Mol. Ther. 15, 2070–9. doi:10.1038/sj.mt.6300311

Son, Y., Cheong, Y.-K., Kim, N.-H., Chung, H.-T., Kang, D.G., Pae, H.-O., 2011. Mitogen-Activated Protein Kinases and Reactive Oxygen Species: How Can ROS Activate MAPK Pathways? J. Signal Transduct. 2011, 792639. doi:10.1155/2011/792639

Strober, W., 2001. Trypan blue exclusion test of cell viability. Curr. Protoc. Immunol. Appendix 3, Appendix 3B. doi:10.1002/0471142735.ima03bs21

Szczubial, M., Kankofer, M., Bochniarz, M., Dąbrowski, R., 2015. Effects of Ovariohysterectomy on Oxidative Stress Markers in Female Dogs. Reprod. Domest. Anim. doi:10.1111/rda.12501

Tesfaye, D., Salilew-Wondim, D., Gebremedhn, S., Sohel, M.M.H., Pandey, H.O., Hoelker, M., Schellander, K., 2017. Potential role of microRNAs in mammalian female fertility. Reprod. Fertil. Dev. 29, 8–23. doi:10.1071/RD16266

Wahid, F., Shehzad, A., Khan, T., Kim, Y.Y., 2010. MicroRNAs: synthesis, mechanism, function, and recent clinical trials. Biochim. Biophys. Acta 1803, 1231–43. doi:10.1016/j.bbamcr.2010.06.013

Wolter, K.G., Hsu, Y.T., Smith, C.L., Nechushtan, A., Xi, X.G., Youle, R.J., 1997. Movement of Bax from the cytosol to mitochondria during apoptosis. J. Cell Biol. 139, 1281–92.

Zhang, M., An, C., Gao, Y., Leak, R.K., Chen, J., Zhang, F., 2013. Emerging roles of Nrf2 and phase II antioxidant enzymes in neuroprotection. Prog. Neurobiol. 100, 30–47. doi:10.1016/j.pneurobio.2012.09.003

Zhang, Y., Tang, L., 2007. Discovery and development of sulforaphane as a cancer chemopreventive phytochemical. Acta Pharmacol. Sin. 28, 1343–1354. doi:10.1111/j.1745-7254.2007.00679.x

Zhao, F., Li, K., Zhao, L., Liu, J., Suo, Q., Zhao, J., Wang, H., Zhao, S., 2014. Effect of Nrf2 on rat ovarian tissues against atrazine-induced anti-oxidative response. Int. J. Clin. Exp. Pathol. 7, 2780–9.